Stratigraphy of the

BURIED TEAYS VALLEY IN WESTERN OHIO AND EASTERN INDIANA

by Tyler A. Norris, T. Andrew Nash, Henry M. Loope, and José Luis Antinao

OPEN-FILE REPORT
2022-2
Columbus 2023

OHIO GEOLOGICAL SURVEY
DEPARTMENT OF NATURAL RESOURCES

INDIANA GEOLOGICAL & WATER SURVEY
INDIANA UNIVERSITY

GRAPHIC DESIGN & LAYOUT: Jeremy E. Gladden
EDITING: Anthony J. Bresnen
FRONT COVER: Rotary sonic drill rig setup (Frontz Drilling) at the site of Willshire-21 boring in Willshire, Ohio.

RECOMMENDED CITATION: Norris, T.A., Nash, T.A., Loope, H.M., and Antinao, J.L., 2023, Stratigraphy of the buried Teays Valley in western Ohio and eastern Indiana: Columbus, Ohio Department of Natural Resources, Division of Geological Survey Open-File Report 2022-2, 30 p. [Revised 2023].

CONTENTS

FIGURES

TABLES

APPENDICES

DATASETS

SELECTED ABBREVIATIONS USED IN THIS REPORT

central age model. . . . . CAM
degrees Celsius. . . . . C°
degrees Fahrenheit . . . . . F°
feet . . . . . ft
grams . . . . . g
gray. . . . . Gy
high density polyethylene . . . . . HDPE
inductively coupled plasma atomic emission spectroscopy . . . . . ICP-AES
inductively coupled plasma mass spectrometry. . . . . ICP-MS
level of detection . . . . . LOD
liters L
mean sea level . . . . . m.s.l.
meters . . . . . m
micrometers . . . . . µm
millimeters. . . . . mm
minimum age model . . . . . MAM
optically stimulated luminescence. . . . . OSL
particle size analysis. . . . . PSA
parts per million . . . . . ppm
plagioclase feldspar . . . . . plag
polyvinyl chloride . . . . . PVC
portable X-ray fluorescence . . . . . pXRF
potassium feldspar . . . . . K-spar
single-aliquot regenerative dose . . . . . SAR
thousand years ago . . . . . ka
x-ray diffraction . . . . . XRD
x-ray fluorescence . . . . . XRF

Stratigraphy of the Buried Teays Valley in western Ohio and eastern Indiana

by
Tyler A. Norris[1], T. Andrew Nash[1],
Henry M. Loope[2], and José Luis Antinao[2]

ABSTRACT

The Ohio Department of Natural Resources, Division of Geological Survey and Indiana Geological and Water Survey have characterized a regional section of the buried Teays-Mahomet (Teays) River Valley system through rotary sonic drilling. The Teays River, once part of a major pre-Quaternary drainage system, was altered and filled with unconsolidated deposits from multiple glacial events. Previous regional mapping efforts in the Teays Valley were limited by the complex and spatially variable nature of the valley's fill, as well as the uncertainty of the valley's local morphology. Passive seismic geophysical methods and preexisting well log data first were used to locate ideal drilling locations within the buried valley in western Ohio and eastern Indiana. Two continuous cores were drilled through the Teays to allow for detailed description of the valley fill stratigraphy and subsampling for physical and geochemical analyses. This report describes the results of the drilling process and subsequent laboratory analyses.

INTRODUCTION

The Teays River System was a major pre-Quaternary Period drainage network with a general flow from the southeast towards the northwest. This system transported surface water from the southern Appalachian Mountains across the lower Great Lakes Region and eventually met with the ancestral Mississippi River in central Illinois (Goldthwait, 1991). This drainage network was likely millions of years old prior to glaciation, developing as a result of uplift along the east coast of North America during the Appalachian Orogeny. This drainage network incised through the Paleozoic bedrock deposited in the Appalachian and Illinois Basins, creating an extensive valley with a main trunk about 1,000 miles long. Multiple glaciations occurred during the Quaternary Period that entirely buried large portions of this paleodrainage network in the lower Great Lakes region and altered the courses of many modern rivers outside of the glaciated area (Teller and Goldthwait, 1991). The modern, buried Teays River Valley contains a complex fill of unconsolidated clay, silt, sand, gravel, and diamicton deposits that vary regionally (Bleuer, 1991). Few studies have managed to effectively characterize the stratigraphy of the Quaternary-aged sediments within the Teays system.

Previous Work

Some of the earliest research on the then-unnamed buried Teays Valley occurred in western Ohio and eastern Indiana. Bownocker (1899) examined the depth to bedrock in the glaciated region near the Ohio-Indiana border and identified the preglacial channel, but he did not study the sediments that filled the preglacial valley. In unglaciated southern Ohio, research detailing terraces, straths, and valley-fill sediments related to the preglacial drainage network originated with Tight (1903). Tight described drainage modifications and lacustrine terrace relationships in southern Ohio and surrounding regions and named the Teays Valley. Later while detailing the effects of glaciation on vegetation in southern Ohio, Wolfe (1942) described the series of events that led to the damming of the Teays River drainage network and

[1] Ohio Department of Natural Resources, Division of Geological Survey, 2045 Morse Rd. Bldg. B-2, Columbus, OH 43229

[2] Indiana Geological & Water Survey, 1001 E. 10th St., Bloomington, IN 47405

the formation of Lake Tight, which resulted in valley filling and terrace carving during a pre-Illinoian glaciation. Work since then has attempted to further define Lake Tight water levels and spatial extent (e.g., Erjavec, 2018).

Many previous studies built upon the drainage history and additional research across the lower Great Lakes region to define further the preglacial drainage network. Stout and others (1943) produced the first published map of the Teays River Valley and preglacial drainage networks for all of Ohio. Horberg's (1945) research connecting the Teays Valley of Ohio with the Mahomet Valley of Illinois completed the regional synthesis of preglacial drainage networks for early twentieth century research and created the modern conceptual understanding of the Teays-Mahomet drainage network. A variety of hypothesized drainage routes across Indiana to connect the Teays and Mahomet Valleys had been proposed by the time detailed bedrock topography mapping was completed for the glaciated portion of the state (Wayne, 1956; Gray, 1982).

Research in the unglaciated portion of Ohio provides sedimentological evidence for Lake Tight. Hoyer (1976) described deposits of exposed sections of the Parker Strath in southern Ohio, which Hoyer interpreted as basal alluvial sediments deposited prior to glaciation, and finer-grained Pleistocene-aged silt and clay lacustrine material (known as Minford Silt or Minford Clay) that accumulated within filled valleys during ice damming. The age of these sediments was further defined from paleomagnetic data in Jacobson and others (1988) and Bonnett and others (1991), revealing that ice damming of the Teays and its former tributaries occurred multiple times, creating several well-defined terrace elevations. While these studies provide insight into the drainage history and early Quaternary chronology of the Teays River Valley, they do not explain the glacial processes nor the timing of those processes that ultimately buried the valley in west-central Ohio and east-central Indiana.

The first significant subsurface investigation of the buried Teays Valley in central Ohio occurred in Madison, Clark, and Champaign Counties (Norris and Spicer, 1958). Boreholes were drilled within the deepest sections of the buried valley following results of geophysical resistivity surveys. Norris and Spicer discovered that in central Ohio, the lowermost deposits within the buried Teays Valley are often ice-dammed lake sediments and typically contain clay, silt, and fine sand. These fine-grained deposits are similar to the Minford Silt deposits found exposed at the surface in southern Ohio but here are overlain by Illinoian- and Wisconsinan-aged glacial tills and outwash (Norris and Spicer, 1958). Norris and Spicer (1958) correlated their basal lake sediments in central Ohio to the Minford Silt of southeast Ohio on the basis of physical characteristics and a maximum elevation of both units at 262 meters (m), or 860 feet (ft), above mean sea level (Tight, 1903; Wolfe, 1942). At its thickest, the Minford Silt is 80.5 m (264 ft) thick at the London Prison Farm in Madison County (Norris and Spicer, 1958). The interpretation of these sediments recovered from test hole borings provided the first strong evidence for the processes that buried the Teays River in Ohio. According to Norris and Spicer (1958), these thick Minford Silt deposits support the hypothesis that ice dammed the river during a pre-Illinoian glaciation near the northernmost reach of the ancient Teays River Valley, probably southwest of Fort Wayne, Indiana. Unfortunately, these boreholes were drilled with rotary drilling methods that did not preserve sediment cores for future analyses to further corroborate these claims. Norris and Spicer's (1958) research in central Ohio partly motivated further study of the valley-fill sediments farther down valley into Indiana.

In Indiana, the first large-scale effort to classify Quaternary-aged, Teays Valley fill through rotary drilling and gamma-ray logging began in 1977 (Bleuer, 1991). Bleuer (1991) synthesizes more than a decade's worth of drilling and gamma-ray logging data to present a comprehensive analysis of the glacial processes and sediments which fill bedrock valleys (Lafayette Bedrock Valley System) in northern Indiana. Included within this analysis is the presentation of a stratigraphic framework that combines mineralogical data and physical properties to classify units from Superior and Grenville provinces down to the member level. These units are correlated across Indiana and into Ohio through comparative analysis of gamma-ray logs collected at wells where samples were not available. Bleuer (1991) interpreted the sequences of sediments that filled the Lafayette Bedrock Valley System and theorized that nine major drainage stages existed within the Lafayette Bedrock Valley System between the onset of

the drainage network and through the Quaternary Period. While this existing stratigraphic framework provides evidence for the sequence of glacial events and processes that buried the Lafayette and Teays systems, there is almost no absolute age control on the sediments that infill these bedrock valleys.

Project Purpose

In this report, we present the first detailed stratigraphic descriptions of the Quaternary-aged sediments that filled the Teays Valley in west-central Ohio and east-central Indiana. Two new rotary sonic cores were collected near Willshire, Ohio (Mercer County) and Domestic, Indiana (Jay County; fig. 1). The Willshire-21 core was collected at 40.691788, -84.773658 from February 23 to February 26, 2021. The Domestic core was collected at 40.546530, -85.079176 from March 2 to March 8, 2021. The stratigraphic descriptions of these cores are supported with geochemical data from portable x-ray fluorescence (pXRF) and x-ray diffraction (XRD), and also particle size analysis (PSA) data through laser diffraction and sieving. Results from these analyses are structured to provide all the raw data collected during this study and to support future research on the Teays Valley in Ohio and Indiana. A brief discussion of how these new cores fit into the historical narrative of the Teays bedrock valley systems follows these results.

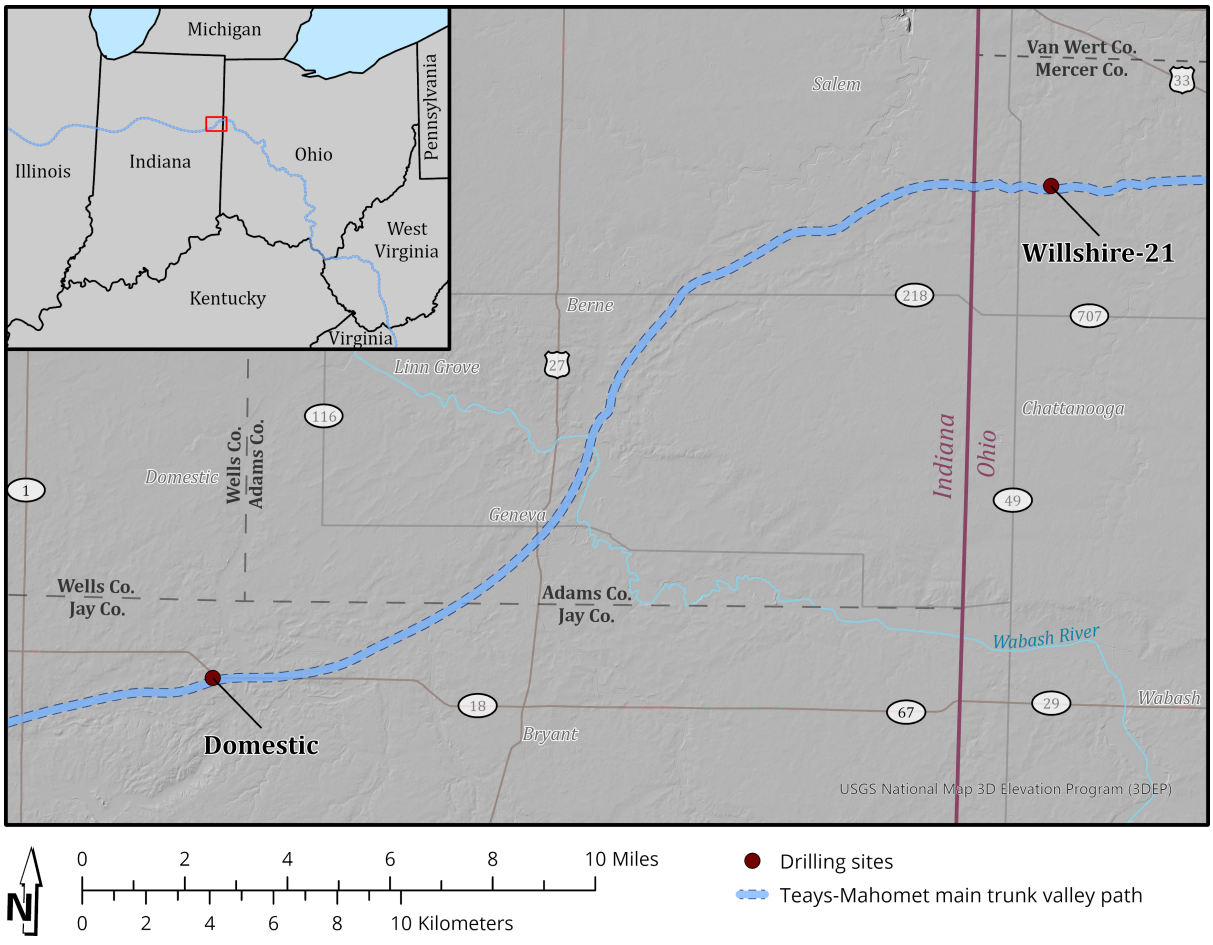

FIGURE 1. Map showing the location of the two drilling sites (Willshire-21 and Domestic; red circles) in relation to the main path of the subsurface Teays-Mahomet Valley (thick light-blue line). The inset map (top) indicates the extent of the location map (red) and shows the regional path (blue) of the main Teays-Mahomet Valley.

METHODS

Drilling and Core Handling

The field sites in close proximity to the buried Teays Valley system were identified by utilizing passive seismic geophysical results obtained while remapping the bedrock topography at the Ohio and Indiana state border (Nash and others, 2021; Rupp and others, 2021). The cores were drilled by Frontz Drilling from Wooster, Ohio. The continuously drilled, 4-inch-diameter sediment cores were bored using a rotary sonic drill rig. The rotary sonic method was chosen because of its ability to reliably recover a continuous, near-undisturbed sediment core compared to other drilling operations, such as air or mud rotary. The typical rotary sonic drilling process is detailed in Figure 2. Extruded 1.5 m (5 ft) core intervals were sheathed into plastic liners and then placed into halved PVC pipes, where they were taped, labeled, and secured for transport. For drilled intervals that were presumed to contain fine-grained sand ideal for Optically Stimulated Luminescence (OSL) dating, 1.5 m (5 ft) core intervals were extruded into black opaque HDPE liners, or were immediately wrapped with black opaque HDPE liners, to prevent exposure to direct light.

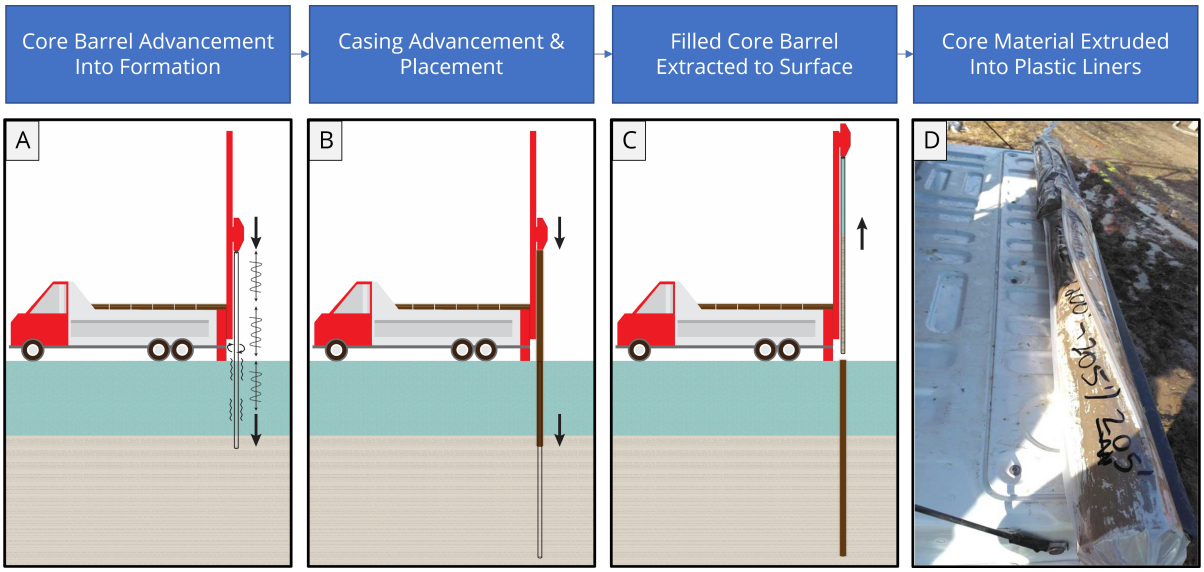

FIGURE 2. Rotary sonic drilling process. A: The core barrel impacts, rotates, and vibrates at a high frequency to penetrate through the subsurface material. B: A casing is drilled to stabilize the hole. C: The filled core barrel is pulled up to the surface. D: The sonic-cored materials are then extracted directly into plastic liners in approximately 1.5 m (5 ft) intervals.

Once the hole was completed and stabilized, the drill strings were removed leaving the empty, cased hole. A tripod with a pulley mount was set up above the hole to allow a Mt. Sopris® 2PGA-1000 gamma sonde to descend the hole, which was controlled by a Matrix logging console and mini-winch. The gamma sonde logged continuously down- and then up-hole using methods described in Bleuer (2004). The gamma logs used in this report were obtained from data gathered up-hole at a rate of 1.5 m/minute (5 ft/minute).

After transport to the H. R. Collins Laboratory and Core Repository in Delaware, Ohio, each 1.5 m (5 ft) section of unconsolidated core was cut and split lengthwise by using a combination of cutting wire, hammers, and putty knives to divide the unconsolidated material into two approximately equal halves. One half was preserved for photography and archiving, and the other half was used for detailed description and subsampling. Archived core halves were placed horizontally onto a core rack stand in groups of sequential 6-m (20-ft) sections (or four drill core runs) for each photo (see **Dataset 1** and **2**). A set of white studio lights was placed on both sides of the core for appropriate lighting, and windows were covered to block ambient light. The photos were taken using a camera mounted on a tripod positioned directly above the core

rack. The remaining non-archived half of the core section was then measured and described by addressing characteristics such as Munsell and general color, lithology, texture, sorting, pebble content, structures, density, contact type, weathering, and secondary features (see **Dataset 3** and **4**). After writing core descriptions, several samples near the center of the core half were obtained, primarily for PSA and pXRF. Samples were taken at regular intervals, especially in diamicton, to obtain at least one sample for PSA and pXRF for every 1.5-m (5-ft) section. Additional samples were taken before and after lithologic contacts. In sections dominated by very coarse sands and gravels, approximately two large grab samples were taken at different intervals per 1.5-m (5-ft) section in lieu of dedicated PSA or pXRF subsamples. Additional samples were taken for potential future X-Ray Diffraction (XRD) and heavy mineral/geochemistry analyses, possible organics, and other instances of unique intervals. After each archival photo was taken and subsamples were collected, both core halves were prepared for long-term storage by sliding each half-PVC core into clear plastic sleeves and taping each end to create an airtight seal.

Portable X-Ray Fluorescence (pXRF)

Elemental abundances were analyzed via pXRF to determine broad chemical similarities and differences of units within the two Teays cores. Methods of unconsolidated sample preparation and analysis for pXRF vary among authors and detail of study (e.g., Wittkop and others, 2020; Knight and others, 2021), but it is largely agreed that the most reliable data are obtained by first preparing the sample and examining only the dry, homogeneous, fine fraction of the matrix materials to avoid effects from heterogenous pebble lithologies, variable grain sizes, and moisture effects, as opposed to measuring directly on the unprocessed sample. The Ohio Geological Survey prepared samples for pXRF analysis by first air drying and then oven drying as needed at approximately 45°C (113°F) to remove excess moisture. The samples were then crushed and powdered via mortar and pestle. These powdered subsamples were then sieved to obtain at least 3 grams of the <0.063-mm fraction. The fine-grained samples were poured and compacted into small polyethylene XRF sample cups with 4-micron-thin plastic film covering the bottom for pXRF analysis.

Each sample's elemental composition estimates were obtained in the lab by measuring sample fluorescence after exposure to X-rays. This analysis was performed using the Ohio Geological Survey's pXRF device (Thermo Scientific Niton XL5 XRF Analyzer) attached to a portable test stand. Each sample was analyzed in mining mode for three batches run at 180 seconds. Each sample's elemental percent values were then converted to oxide percent if applicable (i.e., Al, Ca, Fe, K, Mg, P, Si, and Ti). The sample elemental values were then normalized to two measurements of the NIST standard SRM 2709a (Mackey and others, 2010): one standard analysis was performed before and one performed after a set of sample analyses. The SRM 2709a reference standard was chosen for calibration because its reported composition was expected to have the most geochemical similarity to the tested unconsolidated core samples out of the suite of standards available at the time of analysis. Results of the three normalized sample analyses were then averaged to obtain one set of elemental estimates per sample, expressed in mg/kg (ppm). A propagated uncertainty value was then calculated based on the instrument output of two-sigma values for each reading and the calibration standard error (if available). Note that these uncertainty calculations were performed to provide a relative understanding of error, as pXRF data should be considered a semi-quantitative data source in most situations.

Particle Size Analysis (PSA)

Samples for particle size analysis, processed at the Indiana Geological and Water Survey, were first air-dried and then crushed by mortar and pestle. Two methods were used for particle size analysis. Laser diffraction was used for diamicton (till) samples in determination of the matrix grain size and for silty or sandy samples where the maximum grain diameter was <1.4 mm. Clasts >1.4 mm were removed from till samples by sieving prior to analysis. Particle size distribution was determined using laser diffraction on a Malvern® Mastersizer 3000 (see Miller and Schaetzl, 2012). Samples were dispersed with a 5 g/L solution of sodium metaphosphate and subject to 120 seconds of 40 W inline sonication prior to measurement. Samples were run in triplicate using a Hydro EV wet dispersion unit for 40 seconds each with a stirrer speed of 3,000 revolutions per minute. These three runs were averaged for a final result. Mie scattering with a

particle refractive index of 1.544, a particle absorption index of 1.0, and a dispersant refractive index of 1.33 (water) was used to determine the final grain size distribution (Wiscombe, 1980). Results from laser diffraction analysis are reported in volume percent. Samples with a maximum grain size of >1.4 mm were sieved at 1 phi (ϕ) intervals ($\phi = \log_2 D$, where D = particle diameter in mm), from –7 to 4 phi (128 mm to 0.063 mm) using a sieve shaker. Results from sieving are reported as mass percent.

X-Ray Diffraction (XRD)

Mineralogy of the clay (<2 μm) and silt (8–63 μm) fractions of select diamicton samples were investigated by X-ray diffraction (XRD), following the methods in Jacobs and others (2011). Samples were prepared and analyzed at the XRD laboratory at the University of Wisconsin-Whitewater. Clay was separated by suspension from samples crushed to <2 mm and shaken overnight in a 5% solution of sodium metaphosphate ($NaPO_3$). XRD was completed on clay smears resting on glass slides from 3° to 28° two-θ using Cu-kα radiation, with a scan speed of 2°/minute and a step of 0.02°, using a Rigaku™ Miniflex X-ray diffractometer. Sample treatments include Mg saturation and ethylene glycol solvation, as described in Moore and Reynolds (1989). Selected samples were K-saturated and heated to 350ºC for 1 hour. JADE software (Materials Data Inc.) was used to analyze peak height and background values for the 001 peaks of interest (smectite, vermiculite, illite, kaolinite, and chlorite). Quantification of clay mineral percentages follows a method of the Illinois State Geological Survey (Method I of Hughes and Warren, 1989). Silt minerals were separated by three washings at the appropriate settling time, using a vacuum pump and pipet to withdraw the supernatant (<8 μm); particles >63 μm were separated by sieving. After oven drying, the silt was micronized in a McCrone™ micronizing mill for 2.5 minutes in distilled water, which effectively reduces all particles to <20 μm. XRD was completed on packed powder samples in glass slides and scanned from 25° to 31.5° two-θ using Cu-kα radiation, with a scan speed of 1°/minute and a step of 0.02°. JADE software was used to analyze peak height and background values for quartz, K-feldspar, plagioclase, and dolomite, and mineral percentages were calculated using the methods and mineral intensity factors of Grimley (2000).

Optically Stimulated Luminescence (OSL) Geochronology

Five sediment samples were taken for OSL dating from both Domestic (*n* = 2) and Willshire-21 (*n* = 3) cores. The samples were extracted from sand-and-gravel layers after recovering the core in opaque plastic bags or were subsequently wrapped in opaque liners after recovering core in clear sampling liners with evident sand-and-gravel layers. These cores were then transported to the Indiana Geological and Water Survey laboratories. The outer, exposed sediment was sampled for dose rate measurements, and the inner sediment portion was sampled and processed in controlled light conditions in a room fitted with a sodium-vapor lamp. For dose rate analysis, elemental concentrations were obtained from aliquots of samples that were split, crushed, and pulverized at the Indiana Geological and Water Survey and sent for elemental analysis to an external lab operated by ALS, a private laboratory testing company. Uranium, thorium, and rubidium were measured via Inductively Coupled Plasma Mass Spectrometry (ICP-MS), while % K_2O was measured via Inductively Coupled Plasma Atomic Emission Spectroscopy (ICP-AES; %K_2O was converted into %K for dose rate calculations). Sediment dose rates were based on elemental data corrected for grain size and water content attenuation. The dose rate and age for each sample were calculated from estimated and measured field and laboratory datasets using the online DRAC v1.2 calculator tool (Durcan and others, 2015)[3]. Cosmic dose rates were estimated using the latitude and longitude of sampling sites, elevation, and burial depths as reported in the core logs. The parameters of Prescott and Hutton (1994) were used in these calculations. All aforementioned uncertainties were propagated in quadrature. For OSL analysis, wet sieving was performed on each sample to isolate the 155–255 μm sand fraction, which was subsequently treated with 30% hydrogen

[3] The DRAC tool is available here: https://www.aber.ac.uk/en/dges/research/quaternary/luminescenceresearch-laboratory/dose-rate-calculator. For details, please refer to Durcan and others, 2015.
DRAC v1.2 — Release date: September 2016. DRAC source code is available here: github.com/DRAC-calculator/DRAC-calculator and is licensed under GPLv3).

peroxide (H_2O_2) to remove organic matter and 10% hydrochloric acid (HCl) to remove carbonate minerals. To separate feldspar from quartz and heavy minerals, mineral density separation steps at 2.58 and 2.68 g/cm^3 were completed in 50 mL centrifuge tubes where samples were immersed in a lithium metatungstate ($Li_2O_{13}W_4^{-24}$) solution. Centrifuge tubes were left overnight for sediment to separate, and the sediment separates were subsequently recovered by freezing the tip in liquid nitrogen and decanting the supernatant. The feldspar (<2.58 g/cm^3) and heavy mineral (>2.68 g/cm^3) fractions were archived. Quartz separates were etched in concentrated hydrofluoric acid (HF) for 70 minutes, followed by rinsing 10 times in distilled water, rinsing overnight in HCl, and then followed by a full rinsing to obtain neutrality in water. Clean separates were dried and sieved to 185–255 µm. Some samples required extending the lower grain-size boundary to 85 µm due to low yield of coarser (185–255 µm) grain sizes. The overall effect of increasing the grain-size range is an increase in uncertainty. Some samples had less than 0.5 g remaining after processing (e.g., IGWS-408). Small (2-mm diameter) multigrain aliquots of the 185 to 255 µm fraction were loaded onto stainless steel discs, usually holding 25–40 grains on average, with some discs containing as few as 3–10 grains. After the OSL samples were prepared, a Lexsyg® Smart TL/OSL reader was used for all luminescence measurements, with illumination LEDs at 458 ± 20 nm, operating at 100 mW/cm^2, with filters set to recover light centered at 365 nm. Dose rate calibration for ^{90}Sr beta source, as of January 2021, was 0.131 ± 0.005 Gray/second. The single aliquot regenerative (SAR; Murray and Wintle, 2000) protocol was used on all samples. Growth curves and interpolation to recover the natural burial dose were performed with Analyst® software (individual aliquot growth curves are not shown in this report but available upon request). Instrumental error was set to 5%. Equivalent dose distribution data fitted either a Central Age Model (CAM) or Minimum Age Model (MAM) (Galbraith and others, 1999). The rationale of model preference depends on the sedimentology and inferred depositional environmental setting. A CAM model considers natural variability in the response of quartz to burial doses, which goes beyond what is expected from normal variability in observations of a sample, and it is explained by differences in sensitivity and other luminescence properties of the mineral grains under study. This natural variability is normally quantified by a parameter called *overdispersion* (Galbraith and others, 1999). Equivalent dose distributions and model ages were analyzed with the R Luminescence Package (Fuchs and others, 2013), v. 0.9.21 2023-2-3[4].

RESULTS

Core Stratigraphy

Descriptions of the stratigraphy in both cores show that multiple units of Quaternary-aged sediments are present within the buried valley. Simplified stratigraphic columns for each core show the primary lithology with depth and are compared to select physical and chemical results to determine preliminary interpretations (figs. 3 and 4). The Willshire-21 core has a total depth of 160.7 m (335.0 ft) and the bedrock contact was measured at 100.4 m (329.5 ft). The bedrock elevation at the Willshire-21 drill site was calculated to be 147.7 m (484.5 ft) above mean sea level. The Domestic core has a total depth of 121.9 m (400.0 ft), and the bedrock contact was measured at 119.1 m (390.9 ft). The bedrock elevation at the Domestic drill site was calculated to be 146.0 m (478.9 ft) above mean sea level.

Willshire-21 core stratigraphy

The Willshire-21 core is primarily composed of diamicton, with this material accounting for nearly two-thirds of the total depth of the core (fig. 3). The remaining one-third of the core sediments can be classified either as sand-and-gravel-dominated units interpreted as glaciofluvial packages or as clay-and-silt-dominated units interpreted as glaciolacustrine or lacustrine in origin. Eight major lithologic packages were identified during the description of the Willshire-21 core: four unique diamicton units (A_w, B_w, D_w, and F_w); two dominantly glaciofluvial units (C_w and G_w); one unit dominated by glaciolacustrine with minor glaciofluvial sand and gravels (Unit E_w); and the bottom-most limestone bedrock (Unit H_w).

[4] The R Luminescence package is available here: https://cran.rproject.org/web/packages/Luminescence/.

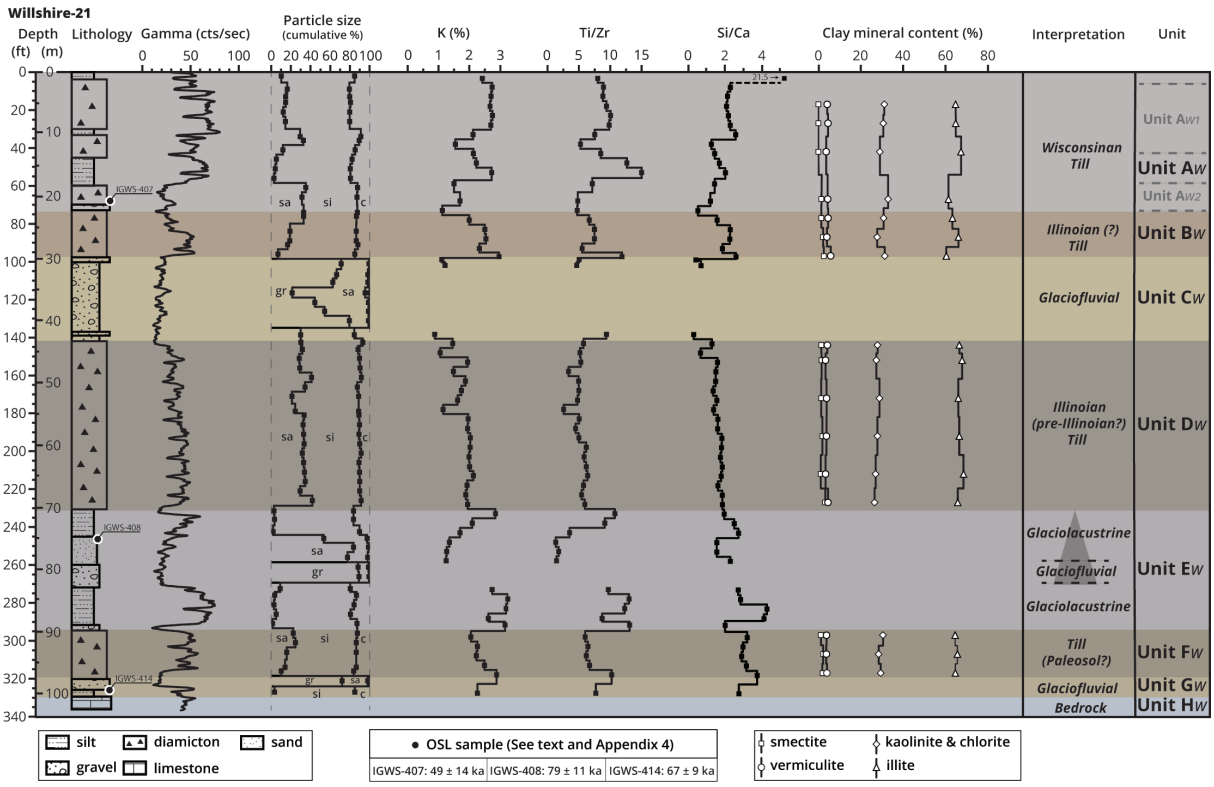

FIGURE 3. Summary of Willshire-21 core stratigraphy with selected results and interpreted units.

Unit A_w. The first diamicton, Unit A_w, is found in the upper 23 m (75 ft) of the core and includes the modern soil developed at the ground surface and several thin silt beds within the diamicton. Where unweathered, this diamicton has a variable gray to grayish brown color (10YR 5/2-1 to 10YR 4/2-4/1). The upper diamicton package (A_{w1}) is homogenous and massive, containing a silty to silty-clay loam matrix that coarsens slightly with depth, with a moderate to abundant clast content. The lowermost diamicton (A_{w2}) within A_w contains a coarser texture and is structureless.

Unit B_w. Directly below Unit A_w is an abrupt, thin silt to fine-sand bed that separates the Unit A_w diamiction and the diamicton in Unit B_w. This diamicton has a unique very dark grayish-brown to brown color (10YR 3/2; dominantly 10YR 4/2) and is relatively thin (about 5.5 m [18 ft] thick). The diamicton in Unit B_w is considerably denser than the diamicton in Unit A_w. Also, Unit B_w contains a coarser matrix (silt to fine sand) compared to Unit A_w (clay to silt) with more abundant >2mm clasts. The lower portion of Unit B_w ends with several interbedded layers of silt and sand.

Unit C_w. The next unit is a coarse, poorly sorted sand-and-gravel package with occasional cobbles. The contact between Unit B_w and Unit C_w is abrupt, denoted by the occurrence of a sand-rich zone. Although much of this unit is composed of massive medium- to coarse-grained sands with angular to subangular clasts, it contains several thin beds of well-sorted sand with minor fining upward and coarsening upward sequences. This coarse unit is 18 m (45 ft) thick and ends with gradational contact that grades into diamicton.

Unit D_w. The third diamicton, Unit D_w, is dark grayish brown (10YR 4/2) with a silty loam textured matrix supporting many angular and subangular pebbles. This unit is the thickest diamicton unit observed in the core (approximately 27 m [90 ft]) and is homogenous with regards to matrix texture and relative clast abundance. This poorly sorted diamicton contains many similarities with the thinner Unit B_w, such as having a dark-brown to gray color (10YR 4/2); moderate gravel and cobble content; high density; and silty matrix texture.

Unit E_w. Beneath the diamicton in Unit D_w is a mix of fine-grained packages and a thinner coarse-grained package, comprising a notable fining upward sequence. The silts and clays within this unit typically have thin laminations and platy structures. Occasional well-sorted fine- to

medium-grain sands do not have any observable bedding and have rounded to subangular grains. A very coarse sand-and-gravel–dominated interval (approximately 4 m [12 ft] thick) marks the beginning of the dominantly fining-upward sequence (between 83 m [272 ft] to 70 m [231 ft]). Below this sand and gravel is an abrupt contact with a clay-and-silt interval similar to the upper portion of this unit, with occasional distorted laminae and thin fine-sand intervals.

Unit F_w. The final, lowermost diamicton exhibits a dark reddish-gray color (5YR 4/2) which grades into a brown color (7.5YR 4/2) after 3 m (10 ft) in depth. The contact is abrupt between Units E_w and F_w. The variably fine-to-coarse matrix is calcareous and has a blocky, massive matrix with many indications of redox and weathered clasts. The fresh material also gave off an organic gaseous odor.

Unit G_w. Underneath Unit F_w is a thin, poorly sorted muddy sand-and-gravel package with a mix of rounded to angular gravels and cobbles. A thin, gravel-rich, very poorly sorted, sandy diamicton-like material transitions into mixed clays and fine sands that composes the end of the unit.

Unit H_w. The bottommost unit contains a mostly weathered and pulverized white to blueish-gray limestone. The contact between Unit G_w and Unit H_w is abrupt, representing the unconformity between the underlying Paleozoic bedrock (likely Ordovician Whitewater Formation, Unit H_w) and the overlying Quaternary-aged unconsolidated sediments (Units A_w–G_w).

Domestic core stratigraphy

The Domestic core is composed primarily of several coarse sand-and-gravel packages and finer sands to silt-and-clay packages, interpreted as transitions between glaciofluvial outwash and glaciolacustrine depositional environments, respectively (fig. 4). Diamicton accounts for only the upper quarter of the entire core. Six major lithologic packages were identified during

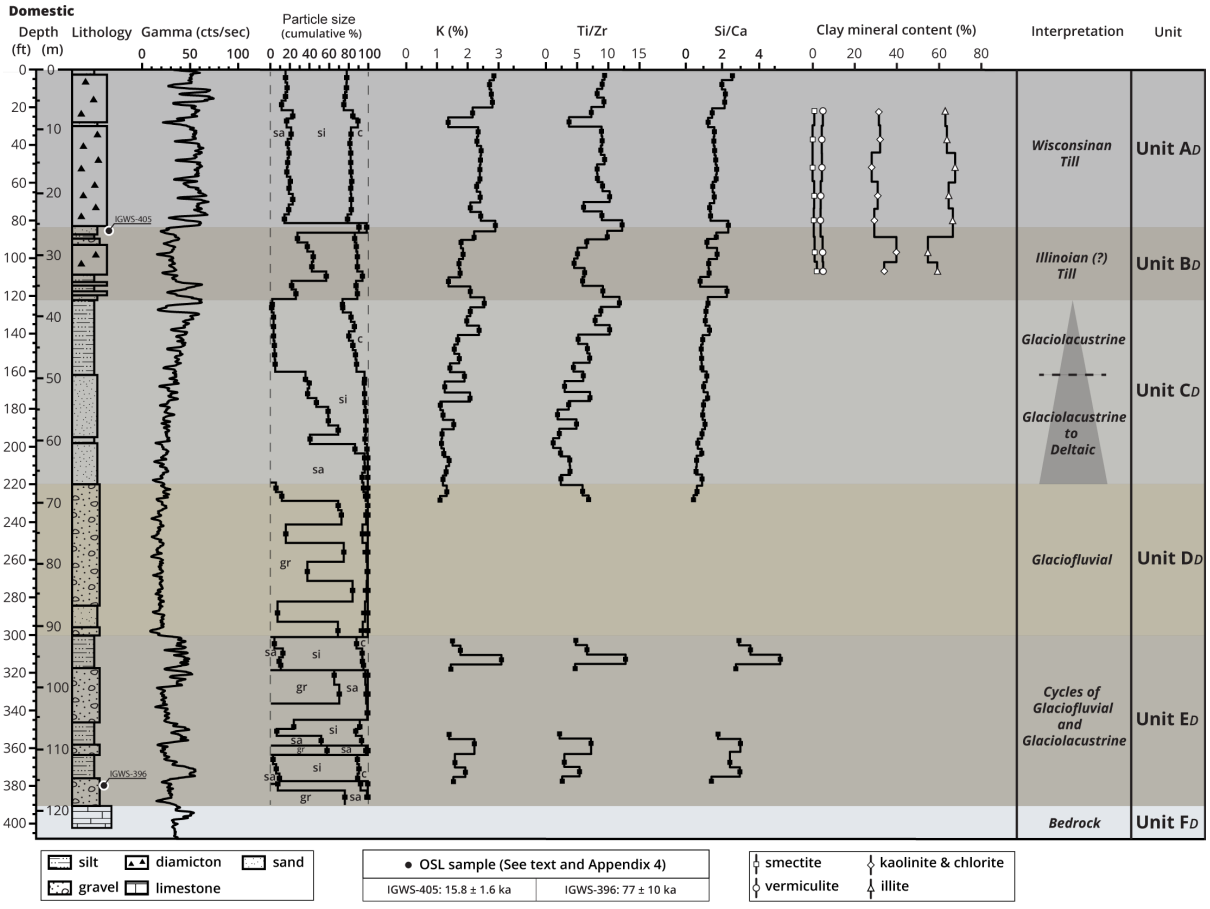

FIGURE 4. Summary of Domestic core stratigraphy with selected results and interpreted units.

the description of the Domestic core: two unique diamicton units (A_D and B_D); one dominantly glaciolacustrine unit with potentially underlying deltaic deposits (C_D); one unit dominated by glaciofluvial sands and gravels (D_D); a mixture between primarily glaciofluvial and glaciolacustrine cycles (E_D); and the bottommost limestone bedrock unit (F_D).

Unit A_D. Unit A_D contains the first diamicton and is found in the upper 26 m (85 ft) of the core; it includes modern soil developed at the ground surface. The upper 6 m (21 ft) of the diamicton contains indications of oxidation and weathering. Below this partially weathered upper portion, the matrix has a dark gray to grayish brown color (10YR 3/1 to 10YR 4/2) and is calcareous. Overall, this diamicton unit has a homogenous silty to silty-clay loam matrix with moderate to abundant clast content with occasional thin beds of silt and fine sand.

Unit B_D. Directly below Unit A_D is Unit B_D, comprising the second and last major diamicton encountered in the core. The contact between Unit A_D and Unit B_D is abrupt, denoted by several feet of tan, fine-to-medium-grained sands and silts. The diamicton in Unit B_D is thinner (approximately 4 m [12 ft]) and notably denser than the overlying diamicton (Unit A_D) and is a very dark-gray color (10YR 3/1 to 10YR 4/1). Unit B_D also contains a massive, coarser matrix (silt to fine sand) with more abundant >2mm clasts compared to the overlying Unit A_D. The lower portion of Unit B_D ends with several interbedded layers of silt and sand.

Unit C_D. The coarser sands at the bottommost section of Unit B_D quickly transition into Unit C_D, a dominantly fine-grained, fining upward sequence dominated by thick clay and silt and fine sands. The upper 12 m (40 ft) of Unit C_D contains homogenous, massive, and calcareous clays and silts (10YR 4/2 to 10YR 4/1). This finer package gradually grades into a coarser silt to fine- to medium-grained sand with depth (about 18 m [58 ft] thick). The sands are massive and very well sorted, occasionally containing thin laminated silty clay layers that alternate colors between laminae (10YR 4/1 and 10YR 3/1). Also within this lower subunit are small packages of coarser sands and trace gravels.

Unit D_D. Unit C_D unevenly grades into Unit D_D, which is approximately 24 m (80 ft) of coarse sand and gravels. This coarse unit is massive with no observable bedding or stratification. Sand-dominated intervals are well sorted and calcareous. Rounded and subrounded pebbles are found all throughout the unit and are dominantly carbonate, shale, or Canadian Shield (igneous/metamorphic) lithologies.

Unit E_D. Unit E_D contains characteristics similar to Unit C_D and Unit D_D but contains a mixture of thinner packages of dominantly fine and dominantly coarse cycles: three silt-clay intervals and three sand-gravel intervals. The contact between E_D and the overlying Unit D_D is considered abrupt (between two core runs). The silt-and-clay intervals are each massive, calcareous, and have a similar dark gray-brown (10YR 4/2) color as Unit C_D. The sand-and-gravel intervals are each moderately sorted, lack bedding, with well-rounded pebbles that are carbonate and Canadian Shield lithologies. However, between 105 m (346 ft) and 106 m (349 ft) there is evidence of a clast-dominated diamicton with a silty matrix. This diamicton separates a coarse and fine sequence, with gradual upper contact (with sand and gravel) and a sharp lower contact (with clay and silt).

Unit F_D. The lowermost unit contains the bedrock contact at a depth of approximately 119 m (391 ft). The contact between the consolidated bedrock and the overlying unconsolidated sand and gravel (Unit E_D) is fairly abrupt, with mostly well-rounded carbonate pebbles and muddy diamicton-like masses found at the base of the unconsolidated. The weathered carbonate bedrock is mostly a white to gray pulverized Upper Ordovician-aged limestone.

pXRF

The calculated estimate of the abundance of the 45 elements was obtained for 112 total sampled intervals (*n* = 57 for Willshire-21; *n* = 55 for Domestic; Appendix 1). For the 45 elements analyzed, 21 elements were consistently below the level of detection for both cores (<LOD; Ag, Au, Bi, Cd, Cl, Co, Hf, Hg, Mo, Nb, Pd, Pr, Re, S, Sb, Se, Sn, Ta, U, W, and Y), and six elements had relatively high percent uncertainty (>30%; Ba, Cr, Mn, Ni, P, and V). Of the remaining 18 elements, three elements typically exhibited highly variable readings among the triplicate analysis for the sample (i.e., the percent difference between readings of the same sample tended to be much greater than the percent uncertainty; Mg, Nd, and Zn). We chose 16 elements to plot and compare for further analysis (fig. 5; Appendix 1; Al, As, Ca, Cu, Ce, Fe, K, La, Mg, Pb, Si, Sr, Rb, Th, Ti, and Zr).

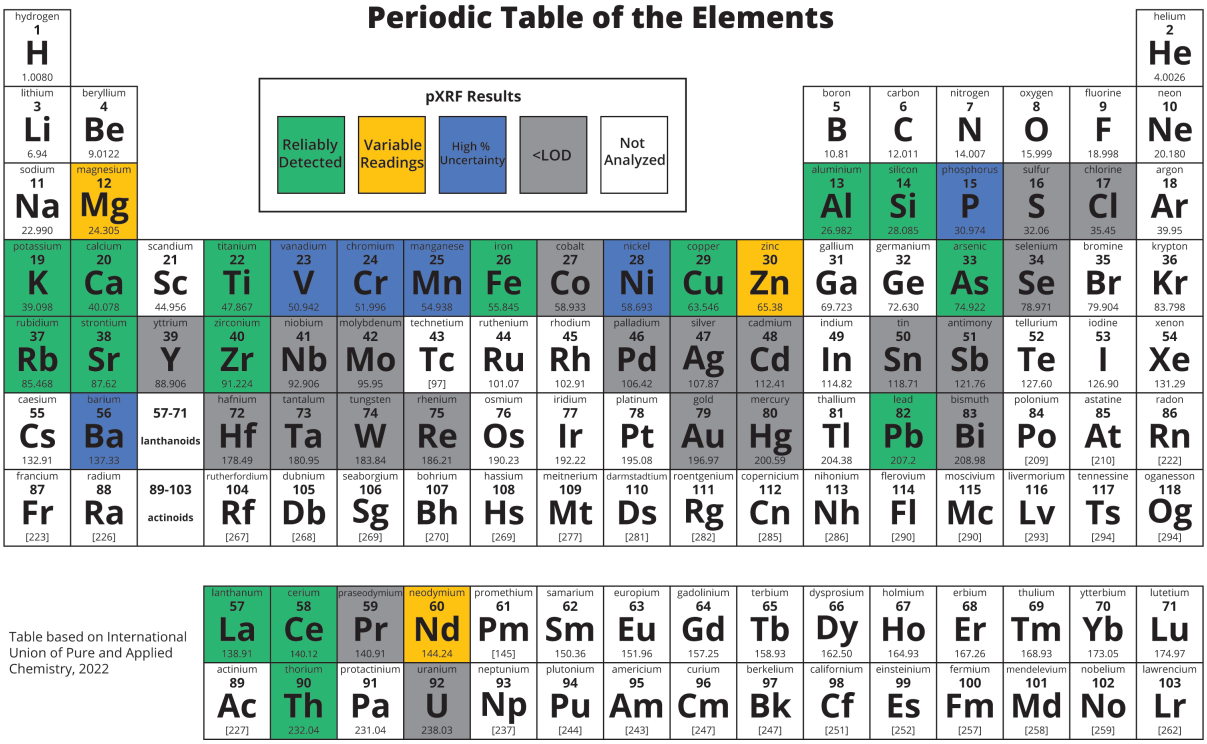

FIGURE 5. Elements visually categorized on a periodic table based on pXRF results. Elements in green were reliably detected and plotted for further analysis. Dark yellow elements had relatively variable readings and were not included for further analysis. Blue elements had high percentages of uncertainty and were not included for further analysis. Gray elements were consistently below the level of detection and were not included for further analysis.

The 16 selected elements can be categorized into several major groups based on elemental abundance. Elements Si and Ca displayed the highest range of abundances overall, generally ranging from >10,000 to >100,000 ppm. Elements with intermediate values (<100,000 ppm) include Al, K, Fe, and Mg. Excluding Ti, which ranged from approximately 500 to 3,000 ppm, the remaining minor elements (Cu, Sr, Zr, As, Ce, La, Pb, Rb, Th) were typically <500 ppm; As, Ce, La, Pb, Rb, and Th were consistently <160 ppm. Both cores displayed similar magnitudes of these elemental abundances but were variable overall.

Although the accuracy of the elemental values obtained from pXRF analysis varies by element and concentration level, the relative change from one sample to the next indicates important trends with depth that can be used in interpretation. While variable in abundance, many elements exhibited similar or conflicting trends with depth, likely based on mineralogy. Broadly, especially in the case of Si and Ca, these associations may be related to dominance in siliciclastic or calcium carbonate source materials with variable contribution to igneous and metamorphic lithologies from eroded and weathered glacial erratics. Many elements mirrored the trends of either Si or Ca. The ratios between some elements may indicate similarities or differences between source materials and may also indicate textural differences. For example, the most homogeneous unit for many elements is Unit D_w in Willshire-21. Unit D_w is the thickest and most uniform till unit with minor variations for most elements, notably Ti/Zr and Si/Ca, implying a consistent parent material homogeneity. The percentage of elements, such as K, compared to the total analysis also follow similar relationships with depth.

PSA

A total of 136 particle size analyses were performed (Willshire-21 *n* = 66; Domestic *n* = 70). These data were plotted as cumulative percent and were categorized by percent gravel, sand, silt, and clay, if applicable. These relative trends aided in unit identification and interpretation. Obvious increases in sand and gravel corresponded to instances of outwash or glaciofluvial

packages, whereas silt-and-clay-dominated samples were mainly from a more glaciolacustrine setting. Grain-size distributions are largely supported by gamma-ray log data, but trends with depth and averages within units provide quantifiable textural information within the sand-silt-clay matrix fraction, especially with diamicton units, that refine and support observations (fig. 6). Diamicton in both cores are mostly determined to be of a silt loam texture, with slight decrease in clay content with depth. Two diamicton intervals in Unit A_w (A_{w1} and A_{w2}) were separated by a notable silt package and were plotted separately to show differences in texture. At a glance, the youngest, uppermost diamicton units (A_{w1} in Willshire-21 and A_D in Domestic) in both cores are texturally similar; but others, such as the sandier unit B_D (in Domestic), appear to be unique. Additional grain size analysis data are found in Appendix 2.

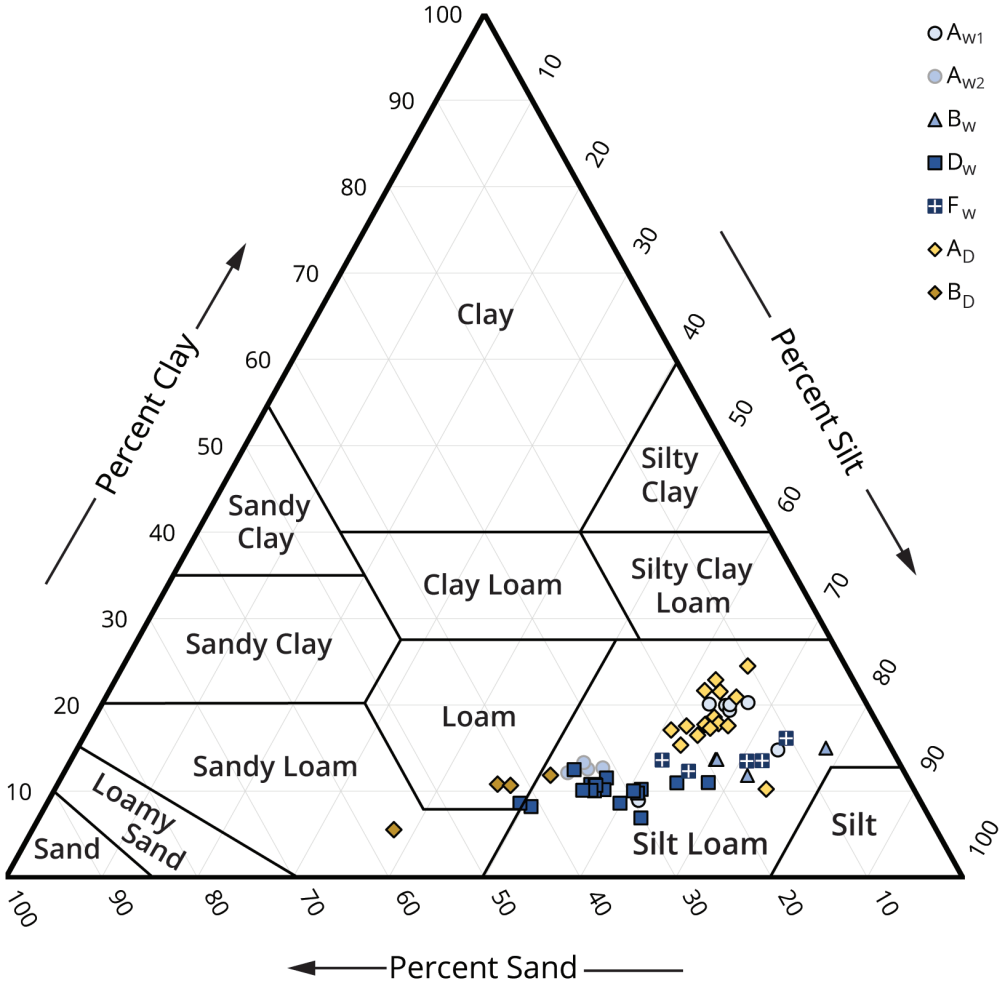

Core	Unit	Top Depth (ft)	Bottom Depth (ft)	Average % Sand	Average % Silt	Average % Clay
Willshire-21	A_{w1}	8.94	40.98	18.31	64.82	16.71
Willshire-21	A_{w2}	60.82	75.98	33.08	54.22	12.70
Willshire-21	B_w	83.94	95.98	15.32	71.13	13.55
Willshire-21	D_w	142.54	225.98	32.03	57.90	10.07
Willshire-21	F_w	295.98	315.98	17.49	68.69	13.82
Domestic	A_D	3.94	78.94	16.86	64.57	18.41
Domestic	B_D	93.61	109.27	44.72	45.53	9.74

FIGURE 6. USDA (United States Department of Agriculture) texture ternary diagram plot of selected PSA samples of major diamicton units (top) and average grain size data for major diamicton units within both cores (bottom). See figures 3 and 4 for stratigraphy and particle information.

XRD

The mineralogy of 23 samples (Willshire-21 *n* = 16; Domestic *n* = 7) within diamicton units were analyzed to determine the mineralogy of the dominantly silt-sized (8–63 μm) and clay-sized (<2 μm) matrix particles. Raw data for the silt fraction were plotted as a percent to determine the amount of quartz, potassium feldspar (K-spar), plagioclase feldspar, calcite, and dolomite for each core (Appendix 3), whereas the percentages of major clay mineral types (smectite, vermiculite, illite, kaolinite, and chlorite) were plotted for the clay fraction (figs. 3 and 4). Diamicton units in both cores appear to have consistent mineralogy with depth. For the silt fraction analysis, quartz and dolomite had the highest abundance in all samples, followed by moderate amounts of calcite and minor components of feldspars. These changes are comparable to slight variations observed in pXRF data. For the clay fraction analysis, illite and chlorite were dominant, with minor amounts of kaolinite, and trace amounts of vermiculite and smectite. The presence of vermiculite is not certain since vermiculite and chlorite share an overlapping peak, which suggests that the analyzed samples were unweathered or potentially the source materials for these clays were also unweathered. Because these data appear to follow similar, relatively unchanging trends between diamicton units with depth, diamicton samples likely originate from the same source area (i.e., the Huron-Erie Lobe).

OSL

Results for quartz OSL dating using the SAR procedure (Murray and Wintle, 2000) are shown in Table 1 and Figures 3 and 4. Many of the aliquots (for example, ~25% of aliquots in sample 396) display slow-medium OSL signal components (Appendix 4, fig. A4-1), which cannot be analyzed using the SAR method and therefore were discarded from further analysis. A large proportion of the remaining aliquots display signal saturation (e.g., Appendix 4, fig. A4-2), indicating their age cannot be estimated given that no finite regeneration dose can reproduce the natural dose given the SAR growth curve. The presence of both saturated aliquots in almost all samples (Appendix A4) along with a population of aliquots with very low equivalent dose values which are not consistent with the stratigraphic framework points to data dispersion that we attribute to sediment being partially bleached during the process of sampling. We therefore consider these ages as minimum ages in Figures 3 and 4.

Table 1. ***Age estimates for analyzed samples along with key data used in calculations.***

Sample ID (IGWS)	Core	Sample depth (feet)	Grain size of analyzed fraction (µm)	K (%)*	Th (ppm)*	U (ppm)*	Water content (wt%)	Cosmic dose rate (Gy/ka)**	Environmental dose rate (Gy/ka)**	Number of aliquots†	Age model§	DE (Gy)#	OSL age (ka)***
396	Domestic	380	180–300	0.78 ± 0.05	2.8 ± 0.5	2.8 ± 0.5	18 ± 5	0 ± 0	1.304 ± 0.091	9 (40)	CAM	100 ± 11	77 ± 10
405	Domestic	85	180–300	0.95 ± 0.05	1.6 ± 0.5	1.1 ± 0.5	18 ± 5	0.023 ± 0.002	1.075 ± 0.087	20 (40)	CAM	17 ± 1.1	15.8 ± 1.6
407	Willshire-21	65	180–255	0.58 ± 0.18	1.7 ± 0.6	1.3 ± 0.5	18 ± 5	0.033 ± 0.003	0.841 ± 0.142	18 (40)	MAM	41 ± 9.1	49 ± 14
408	Willshire-21	245	125–180	0.74 ± 0.05	4.4 ± 0.5	1.7 ± 0.5	18 ± 5	0.004 ± 0	1.183 ± 0.089	20 (40)	CAM	94 ± 11	79 ± 11
414	Willshire-21	325	180–300	0.89 ± 0.05	3.3 ± 0.5	2.3 ± 0.5	18 ± 5	0.004 ± 0	1.319 ± 0.091	9 (40)	CAM	88 ± 10	67 ± 9

*Radioelemental determination conducted using inductively coupled plasma–mass spectrometry and inductively coupled plasma–optical emission spectrometry techniques.

**Cosmic dose rate calculated following Prescott and Hutton (1994). Both cosmic and total dose rate calculated using the Dose Rate and Age online calculator (Durcan et al., 2015).

†Number of aliquots used in age calculation and total number of aliquots measured in parentheses.

§Central Age Model (CAM) and Minimum Age Model (MAM) from Gailbraith and others, 1999.

#Equivalent dose (DE) calculated using specified age model.

***Age analysis using single-aliquot regenerative-dose method (SAR, Murray and Wintle, 2000).

DISCUSSION

The addition of the Domestic and Willshire-21 cores helps to expand the established regional stratigraphic framework of the Lafayette and Teays systems. Sediments preserved within the valley span multiple glacial episodes and therefore represent a more complete account of regional glacial history, relative to nearby upland areas. A comparison of the core stratigraphy with relation to previously published models of the bedrock surface further depict the differences in valley fill and morphology (figs. 7 and 8). This complex glacial history is evidenced by the remarkably differing unconsolidated sediment packages between the two cores. Willshire-21 contains dominantly diamicton units with relatively thin lacustrine and outwash units, whereas Domestic contained less diamicton overall but is dominated by several thicker sequences of glaciolacustrine and outwash. These findings confirm that the buried bedrock system is filled with inconsistent unconsolidated deposits that vary even within a span less than 32 kilometers (20 miles). Within the study area, the eastern portion of the valley (Willshire-21) contains strong evidence of glaciogenic materials directly deposited by ice (i.e., tills), whereas the western portion of the valley (Domestic) contains more evidence of materials deposited by water (i.e., glaciofluvial sands and gravels and silts and clays related to suspension settling). This evidence refines the subglacial-proglacial transition interpretation from Bleuer (1991), which suggests lake ice-damming at bends in the valley near the Ohio-Indiana state border (i.e., the Marion Valley section). Continued drilling with additional physical, chemical, and age data within the buried Teays system is needed to fully detail correlations between cores and regional glacial frameworks.

CONCLUSIONS AND FUTURE WORK

The data presented in this report provide additional evidence for the variable nature of the buried Teays-Mohamet Valley fill and can be used to support detailed Teays stratigraphy and regional Quaternary studies in the future. Future works can correlate the upper till units and some of the glaciolacustrine and glaciofluvial events into a regional framework. Much of the Teays Valley fill is unique between these two borings, and the unit sequences also differ from previous core stratigraphy works within the Teays. These findings warrant a more detailed analysis of not only the material recovered from this project, but the need for additional deep borings within the Teays.

Future studies could more rigorously test physical and chemical properties of the Willshire-21 and Domestic cores to support regional Quaternary stratigraphic frameworks and an in-depth understanding of the Teays Valley history. Continued work on elemental data can identify trends with other core characteristics by running more samples with other analysis techniques, such as conventional X-Ray Fluorescence (XRF) and ICP-MS. The pXRF data provided in this report may help guide desired target zones for such analyses. The XRD data obtained during this project suggests consistent source material for diamicton units, but continued stratigraphic analysis is needed to correlate these tills in a regional context. Geochemical data combined with particle size data can aid in the classification of till units and glacial events. Such glacial events can be interpreted with age constraints through additional age-dates from OSL dating, radiocarbon dating, and other techniques. OSL samples processed for this project represent minimum ages due to partial bleaching issues introduced during sampling. Additional geochronologic analyses would be required to develop an absolute age model for the deposition of Quaternary sediments into the Teays Valley. The data presented in this report are intended to provide a reference and guide for future work to understanding the Teays Valley development and regional glacial history.

ACKNOWLEDGEMENTS

The authors thank the Great Lakes Mapping Coalition (Cooperative Agreement Number G20AC00302) for the funds and opportunity to work on the project. The completion of this report was possible with support from the Ohio and Indiana State Geologists. We also thank staff who assisted with the project during drilling, core handling, and sample prep and analysis, including but not limited to: Jeffery Deisher (ODNR), Brittany Parrick (ODNR), Samuel Hulett (ODNR), and Thomas Valachovics (ODNR). Peter Jacobs (University of Wisconsin-Whitewater) prepared and analyzed XRD samples for clay and silt mineralogy. Special thanks go to the landowners who allowed drilling on their properties and to the drill crew at Fronz Drilling who efficiently drilled for many days and accommodated us in the field.

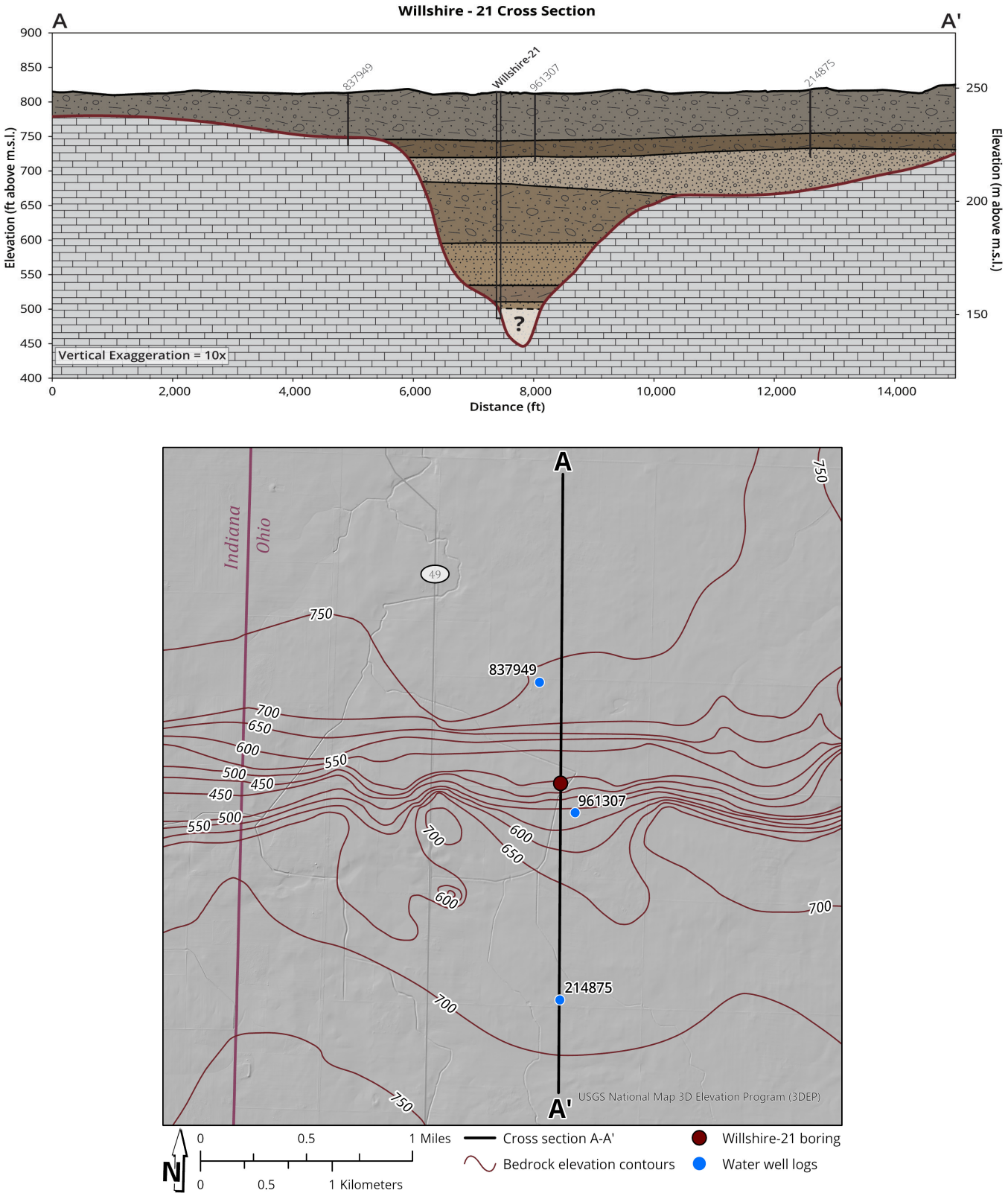

FIGURE 7. Cross section of Willshire-21 based on major stratigraphic units (top) and reference map (bottom). Bedrock surface contact modeled from previous mapping efforts (Rupp and others, 2021; Nash and others, 2021). The bottommost section of the buried Teays valley (thalweg) was not drilled through and is lacking lithologic information ("?") but is inferred to be composed of sand-and-gravel similar to Unit Gw. Reliable water wells within approximately 305 m (1,000 ft) perpendicular to the cross-section line are labeled by record number (ODNR, 2022).

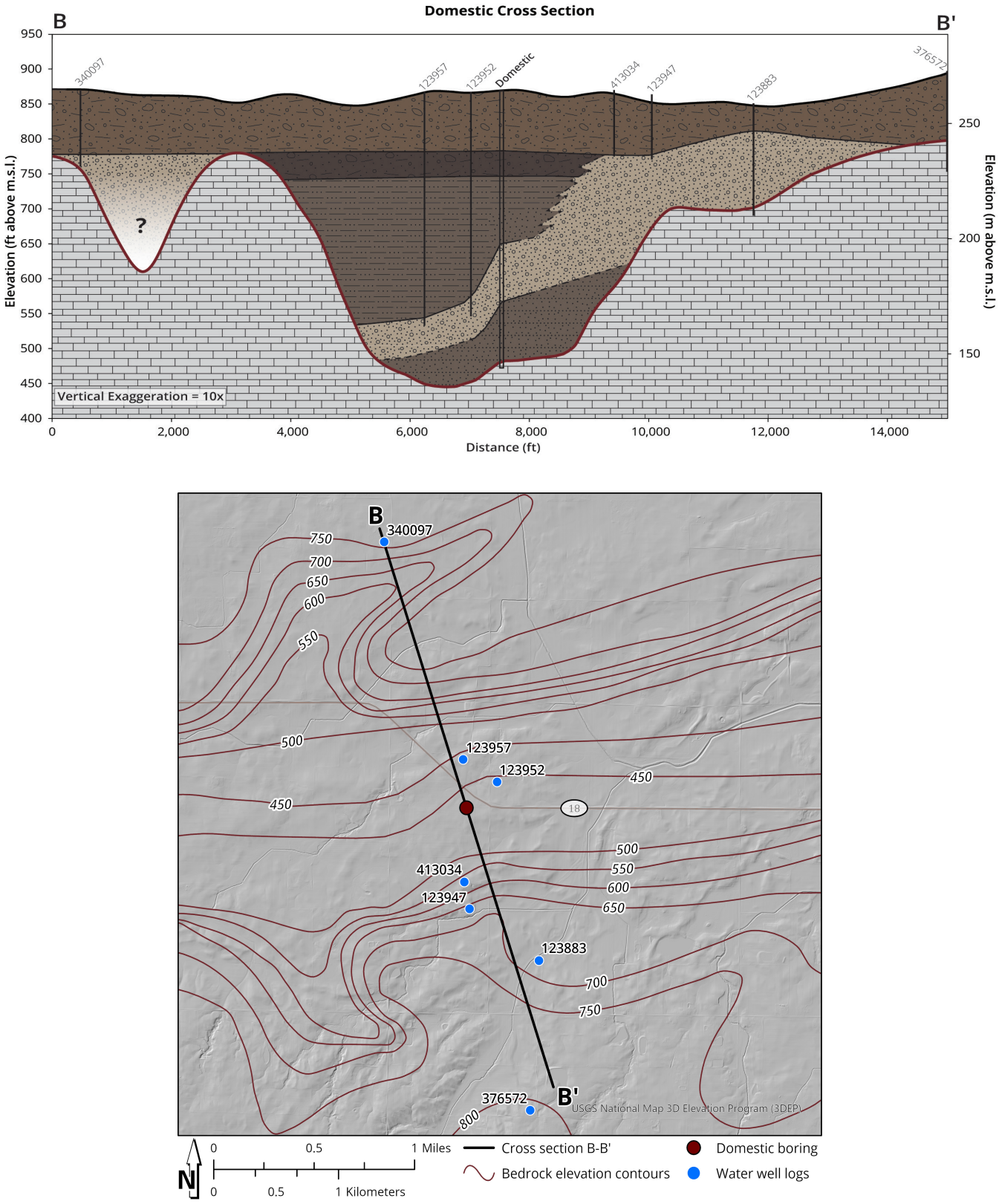

FIGURE 8. Cross section of Domestic based on major stratigraphic units (top) and reference map (bottom). Bedrock surface contact modeled from previous mapping efforts (edited from Rupp and others, 2021). The modelled buried valley to the northwest of the Domestic boring is lacking lithologic information ("?") but may be filled with sand-and-gravel based on the nearby well log (ID 340097). Reliable water wells within approximately 305 m (1,000 ft) perpendicular to the cross-section line are labeled by record number (IDNR, 2019).

REFERENCES

Bleuer, N.K.,1991, The Lafayette Bedrock Valley System of Indiana; concept, form, and fill stratigraphy, *in* Melhorn, W.N., and Kempton, J.P., eds., Geology and hydrogeology of the Teays-Mahomet Bedrock Valley System: Geological Society of America Special Paper 258, Boulder, Colorado, p. 51–77.

Bleuer, N.K., 2004, Slow-logging subtle sequences–the gamma-ray log character of glaciogenic and other unconsolidated sedimentary systems: Indiana Geological Survey Special Report 65, 39 p.

Bonnett, R.B., Noltimier, H.C., and Sanderson, D.D., 1991, A paleomagnetic study of the early Pleistocene Minford Silt Member, Teays Formation, West Virginia, *in* Melhorn, W.N., and Kempton, J.P., eds., Geology and hydrogeology of the Teays-Mahomet Bedrock Valley System: Boulder, Colorado, Geological Society of America Special Paper 258, p. 9–18.

Bownocker, J.A., 1899, A deep pre-glacial channel in western Ohio and Eastern Indiana: The American Geologist vol. 23, p. 178–182.

Buylaert, J.P., Jain, M., Murray, A.S., Thomsen, K.J., Thiel, C., and Sohbati, R., 2012, A robust feldspar luminescence dating method for Middle and Late Pleistocene sediments: Boreas, v. 41, no. 3, p. 435–451.

Durcan, J.A., King, G.E., Duller, G.A,T., 2015, DRAC—Dose rate and age calculator for trapped charge dating: Quaternary Geochronology, v. 28, p. 54–61. doi:10.1016/j.quageo.2015.03.012.

Erjavec, J.L., 2018, A new map of Pleistocene proglacial Lake Tight based on GIS modeling and analysis: Ohio Journal of Science v. 118, no. 2, p. 57–65. http://dx.doi.org/10.18061/ojs.v118i2.6548

Fuchs, M.C., Kreutzer, S., Burow, C., Dietze, M., Fischer, M., Schmidt, C., Fuchs, M., 2015. Data processing in luminescence dating analysis—An exemplary workflow using the R package 'Luminescence'. Quaternary International, v. 362,p. 8–13. https://doi.org/10.1016/j.quaint.2014.06.034

Galbraith, R.F., Roberts, R.G., Laslett, G.M., Yoshida, H., and Olley, J.M., 1999, Optical dating of single and multiple grains of quartz from Jinmium rock shelter, northern Australia—Part I, experimental design and statistical models: Archaeometry, v. 41, no. 2, p. 339–364.

Goldthwait, R.P., 1991, The Teays valley problem: a historical perspective, *in* Melhorn, W.N. and Kempton, J.P., eds., Geology and hydrogeology of the Teays-Mahomet Bedrock Valley System: Geological Society of America Special Paper 258, Boulder, Colorado, p. 3–8.

Gray, H.H., 1982, Map of Indiana showing topography of the bedrock surface: Indiana Geological Survey, Miscellaneous Map 35, scale 1:500,000.

Grimley, D.A., 2000, Glacial and nonglacial sediment contributions to Wisconsin Episode loess in the central United States: Geological Society of America Bulletin 112, p. 1475–1495.

Horberg, L., 1945, A major buried valley in East-Central Illinois and its regional relationships: The Journal of Geology v. 53, no. 5, p. 349–361.

Hoyer, M.C., 1976, Quaternary valley fill of the abandoned Teays drainage system in southern Ohio: Columbus, The Ohio State University, Ph.D dissertation, 163 p.

Hughes, R.E., Warren, R., 1989, Evaluation of the economic usefulness of earth materials by X-ray diffraction *in* Hughes, R.E., Bradbury, J.C. (eds.), Proceedings of the 23rd Forum on Geology of Industrial Minerals: Illinois State Geologic Survey, Mineral Notes 102, p. 47–57.

Indiana Department of Natural Resources, Division of Water, Resource Assessment Section (IDNR), 2019, WATERWELLS_IDNR_IN.SHP: Water well locations in Indiana: 1:24,000, point shapefile.

Knight, R.D., Kjarsgaard, B.A., and Hazen R.A.J., 2021, An analytical protocol for determining the elemental chemistry of Quaternary sediments using a portable X-ray fluorescence spectrometer: Applied Geochemistry, v. 131, 15 p.

Jacobs, P.M., Mason, J.A., and Hanson, P.R., 2011, Mississippi Valley regional source of loess on the southern Green Bay Lobe land surface, Wisconsin: Quaternary Research, v. 75, p. 574–583.

Jacobson, R.B., Elston, D.P., and Heaton, J.W., 1988, Stratigraphy and magnetic polarity of the high terrace remnants in the Upper Ohio and Monongahela Rivers in West Virginia, Pennsylvania, and Ohio: Quaternary Research, v. 29, p. 216–232.

Mackey, E.A., Christopher, S.J., Lindstrom, R.M. , Long, S.E., Marlow, A.F., Murphy, K.E., Paul, R.L., Popelka-Filcoff, R.S, Rabb, S.A., Sieber, J.R., Spatz, R.O., Tomlin, B.E., Wood, L.J., Yen, J.H., Yu, L.L., R. Zeisler, Wilson, S.A., Adams, M.G., Brown, Z.A., Lamothe, P.L., Taggart, J.E., Jones, C., and Nebelsick, J., 2010, Certification of three NIST renewal soil standard reference materials for element content—SRM 2709a San Joaquin Soil, SRM 2710a Montana Soil I, and SRM 2711a Montana Soil II: National Institute of Standards and Technology, Gaithersburg, Maryland, NIST Special Publication 260-172.

Miller, B.A., and Schaetzl, R.J., 2012, Precision of soil particle size analysis using laser diffractometry: Soil Science Society of America Journal, v. 76, p. 1719–1727.

Moore, D.M., and Reynolds, Jr., R.C., 1989, X-ray diffraction and the identification and analysis of clay minerals: Oxford University Press, 322 p.

Murray, A.S., Wintle, A.G., 2000, Luminescence dating of quartz using an improved single-aliquot regenerative-dose protocol: Radiation Measurements, v. 32, iss. 1, p. 57–73.

Nash, T.A., Norris, T.A., Rupp, R.F., Tripp, D.C., Antinao, J.L., and Loope, H.M., 2021, Bedrock topography of the Willshire 7.5-minute quadrangle, Ohio-Indiana: Columbus, Ohio Department of Natural Resources, Division of Geological Survey Digital Map Series SG-4B, scale 1:24,000.

Norris, S.E., and Spicer, H.C., 1958, Geological and geophysical study of the preglacial Teays Valley in west-central Ohio, *in* Contributions to the Hydrology of the United States 1956–1959: Washington, U.S. Geological Survey, Water-Supply Paper 1460, 435 p.

Ohio Department of Natural Resources Division of Geological Survey, 2022, Water Wells Database, last accessed June 30, 2022 at <https://waterwells.ohiodnr.gov>.

Prescott, J.R. and Hutton, J.T., 1994, Cosmic ray and gamma ray dosimetry for TL and ESR: Nuclear Tracks and Radiation Measurements, v. 14, p. 223–227.

Prescott, J.R. and Hutton, J.T., 1994, Cosmic ray contributions to dose rates for luminescence and ESR dating—large depths and long-term time variations: Radiation Measurements, v. 23, p. 497–500.

Rupp, R.F., Tripp, D.C., Antinao, J.L., Loope, H.M., Johnson, M.R., Nash, T.A., and Norris, T.A., 2021, Bedrock elevation of the Berne, Domestic, Geneva, and Willshire 7.5-minute quadrangles, Indiana-Ohio: Indiana Geological and Water Survey, Indiana Journal of Earth Sciences, v. 3, scale 1:48,000. doi: 10.14434/ijes.v3i1.31742.

Stout, Wilber, Ver Steeg, Karl, and Lamb, G.F., 1943, Geology of water in Ohio: Columbus, Ohio Department of Natural Resources, Division of Geological Survey Bulletin 44, 694 p.

Teller, J.T., and Goldthwait, R.P., 1991, The Old Kentucky River; A major tributary to the Teays River, *in* Melhorn, W.N., and Kempton, J.P., eds., Geology and hydrogeology of the Teays-Mahomet Bedrock Valley System: Geological Society of America Special Paper 258, Boulder, Colorado, p. 29–41.

Tight, W.G., 1903, Drainage modifications in southeastern Ohio and adjacent parts of West Virginia and Kentucky: U.S. Geological Survey Professional Paper 13, 111 p.

Udden, J.A., 1914, Mechanical composition of clastic sediments: Geological Society of America Bulletin v. 25, no. 1, p. 655–744.

Wayne, W.J., 1956, Thickness of drift and bedrock topography of Indiana north of the Wisconsin glacial boundary: Indiana Geological Survey Progress Report 7, 70 p.

Wentworth, C.K., 1922, A scale of grade and class terms for clastic sediments: The Journal of Geology, v. 30, no. 5, p. 377–392.

Wiscombe, W.J., 1980, Improved Mie scattering algorithms: Applied Optics, v. 19, p. 1505–1509.

Wittkop, C., Bartley, J.K., Krueger, R., Bouvier, A., Georg, R.B., Knaeble, A.R., St. Clair, K., Piper, C., Breckenridge, A., 2020, Influence of provenance and transport process on the geochemistry and radiogenic (Hf, Nd, Sr) isotopic composition of Pleistocene glacial sediments, Minnesota, USA: Chemical Geology, v. 532, 17 p.

Wolfe, J.N., 1942, Species isolation and a proglacial lake in southern Ohio: Ohio Journal of Science, v. 42, p. 2–12.

This page intentionally left blank

Table A1-1. ***Willshire-21 pXRF table showing calculated average elemental values and associated uncertainties with depth.***

Core	Depth (m)	Depth (ft)	Al	Al +/-	As	As +/-	Ba	Ba +/-	Ca	Ca +/-	Ce	Ce +/-	Cr	Cr +/-	Cu	Cu +/-	Fe	Fe +/-	K	K +/-	La	La +/-	Mg	Mg +/-	Mn	Mn +/-	Nd	Nd +/-	Ni	Ni +/-	P	P +/-	Pb	Pb +/-	Rb	Rb +/-	Si	Si +/-	Sr	Sr +/-	Th	Th +/-	Ti	Ti +/-	V	V +/-	Zn	Zn +/-	Zr	Zr +/-
Willshire-21	1.00	3.28	36875.82	1235.41	19.09	4.00	566.79	405.16	6546.22	325.38	46.96	7.18	97.64	54.27	149.45	30.30	31694.83	685.43	24227.90	738.36	22.73	3.66	5081.06	1362.40	513.54	528.14	17.79	2.11	58.60	10.68	201.13	70.29	27.58	1.98	143.80	5.14	140541.92	1989.28	133.89	3.62	12.72	2.11	2814.58	178.43	146.36	62.15	165.58	9.79	352.69	83.28
Willshire-21	2.42	7.95	38685.22	1384.02	14.64	3.30	591.87	422.91	54777.40	2628.28	51.48	7.71	63.26	46.91	98.42	21.01	26181.90	570.84	27360.43	829.83	26.93	4.10	10047.07	2249.49	478.44	520.00	22.63	2.47	46.50	10.01	154.21	71.84	20.25	1.62	123.15	4.55	126397.74	1820.89	210.23	5.50	9.54	1.82	2284.18	153.76	111.36	52.24	163.62	9.70	256.50	60.58
Willshire-21	3.85	12.62	40328.04	1454.76	11.45	2.84	444.38	317.52	60004.74	2877.78	29.10	5.78	77.52	47.26	155.28	31.39	23410.68	512.07	27009.75	818.33	13.40	2.98	10895.04	2419.97	420.36	485.36	10.85	1.74	37.29	9.57	201.40	81.64	19.20	1.57	119.46	4.45	129124.59	1862.59	220.40	5.76	10.90	1.94	2171.12	146.67	111.06	50.57	153.42	9.24	245.43	57.96
Willshire-21	5.47	17.95	35918.56	1310.78	12.60	3.30	536.82	383.99	57927.88	2779.03	45.97	6.88	58.40	45.84	86.29	17.76	24222.60	529.20	26699.65	809.61	23.70	3.85	9748.23	2114.98	<LOD	<LOD	18.51	2.14	42.62	9.48	167.16	73.02	26.88	1.94	121.93	4.53	121574.71	1760.22	251.56	6.54	9.54	1.82	2207.31	149.87	113.02	54.33	171.08	10.04	235.45	55.60
Willshire-21	7.00	22.95	37964.27	1365.70	14.00	3.52	533.31	381.29	55890.85	2681.77	40.43	6.40	92.62	51.69	267.78	49.92	24854.82	542.71	27495.64	833.37	21.70	3.64	10019.84	2137.45	441.81	513.32	16.48	2.00	48.24	9.77	199.50	75.19	22.69	1.73	126.03	4.65	122660.71	1773.31	248.03	6.45	9.08	1.78	2180.73	150.31	138.73	61.43	201.68	11.81	217.04	51.26
Willshire-21	8.52	27.95	35842.22	1289.98	13.30	3.41	496.86	355.33	54629.26	2621.34	38.76	6.27	68.44	46.83	55.47	11.85	24524.66	535.18	26963.13	817.58	20.76	3.57	8306.76	1904.97	<LOD	<LOD	15.28	1.90	51.52	9.94	191.38	74.59	15.36	1.40	124.54	4.61	125390.00	1806.91	235.47	6.14	9.54	1.82	2247.07	151.56	111.11	53.87	107.90	7.31	228.76	54.02
Willshire-21	10.04	32.95	30594.71	1149.62	17.50	4.12	310.03	221.61	52529.37	2520.84	15.25	4.49	57.54	42.28	262.98	49.06	25688.31	559.56	21184.52	646.41	6.88	2.49	10524.68	2255.75	492.44	520.82	5.45	1.35	30.41	8.84	191.86	72.99	21.60	1.73	93.91	3.25	135897.43	1947.56	208.78	5.47	8.18	1.71	2266.02	149.99	91.07	52.09	186.38	10.74	301.86	71.29
Willshire-21	11.57	37.95	26387.03	1078.21	11.90	3.19	493.64	353.02	89103.81	4270.27	53.39	7.54	48.42	35.10	63.01	13.77	16846.55	373.81	15416.64	474.18	29.87	4.42	17554.34	3250.83	<LOD	<LOD	24.33	2.45	17.05	7.12	81.19	60.92	25.92	1.95	60.72	2.27	114686.43	1679.28	233.11	6.08	4.54	1.48	1573.16	112.78	77.43	43.96	114.97	7.59	299.11	70.66
Willshire-21	13.09	42.95	34495.67	1316.47	12.60	3.30	548.97	392.63	80744.18	3870.43	58.09	7.99	<LOD	<LOD	308.18	57.15	19830.93	436.89	22292.04	648.47	31.17	4.50	15961.00	3055.75	404.71	472.59	25.00	2.50	19.35	7.19	183.69	73.22	29.52	2.14	90.14	3.13	118075.96	1721.98	354.77	9.15	6.36	1.58	1895.08	130.33	82.88	47.82	116.54	7.66	223.64	52.82
Willshire-21	14.62	47.95	33827.12	1278.94	10.50	2.49	512.66	366.48	70513.49	3380.44	51.46	7.63	62.90	42.58	53.68	12.33	21383.95	469.60	22245.38	676.52	27.42	4.11	16913.92	3481.43	<LOD	<LOD	21.84	2.41	29.04	8.49	148.17	71.98	20.44	1.73	101.28	3.47	120411.94	1748.05	212.84	5.57	7.72	1.68	1873.57	131.62	107.48	56.73	101.63	6.82	148.15	35.00
Willshire-21	16.14	52.95	38738.06	1395.36	9.33	2.36	548.80	392.48	58646.29	2813.08	44.32	6.91	62.17	45.28	125.01	24.99	25121.23	548.29	27225.21	823.83	24.40	3.82	13593.66	2953.76	<LOD	<LOD	19.38	2.23	46.36	9.67	134.49	68.00	20.44	1.73	131.62	4.83	119390.61	1727.83	285.23	7.39	8.63	1.75	2133.98	145.41	131.21	65.25	127.92	8.13	142.26	33.61
Willshire-21	17.96	58.94	25240.73	1041.11	15.17	3.11	485.35	346.91	83067.34	3980.09	60.43	8.47	<LOD	<LOD	129.95	25.87	19692.95	433.87	14970.74	460.91	30.85	4.45	16702.37	3506.82	<LOD	<LOD	27.02	2.78	14.05	7.17	156.24	74.86	22.30	1.82	64.10	2.37	121076.61	1760.61	228.57	5.97	5.45	1.53	1767.03	122.62	60.75	42.53	81.62	5.51	248.23	58.60
Willshire-21	20.71	67.95	25204.20	1061.62	10.18	2.68	446.42	319.25	91779.41	4398.00	50.00	8.08	42.15	33.02	78.18	14.69	16886.89	373.53	16926.93	518.87	25.42	3.94	16241.20	3312.84	425.73	476.24	20.56	2.27	17.71	7.83	116.06	64.20	25.48	1.87	64.16	2.35	113369.40	1666.35	327.95	8.47	5.45	1.53	1503.52	111.37	71.36	40.58	90.39	5.82	311.11	73.51
Willshire-21	22.24	72.95	17946.53	940.67	8.27	2.45	312.06	223.26	151180.79	7241.48	37.41	7.03	35.41	28.51	282.81	47.21	13258.63	298.10	11198.41	350.02	17.75	3.33	24226.42	4706.48	427.00	460.24	15.38	1.98	<LOD	<LOD	125.73	70.16	24.79	1.84	35.77	1.60	85775.67	1324.02	355.79	9.39	2.27	1.39	802.07	81.21	52.62	33.52	116.38	7.59	170.00	40.16
Willshire-21	23.76	77.95	31119.98	1224.58	13.36	3.11	483.85	345.67	78883.41	3781.49	58.24	8.92	<LOD	<LOD	71.46	13.75	18291.93	403.47	19923.30	607.95	27.88	4.15	15501.06	3177.98	500.07	516.81	22.51	2.41	21.76	7.96	156.21	66.57	14.66	1.38	77.06	2.72	125673.70	1826.90	387.89	10.12	5.90	1.56	1823.45	127.41	84.84	45.89	73.32	5.15	274.44	64.87
Willshire-21	25.28	82.95	41307.50	1469.14	14.64	3.30	537.99	384.47	55839.74	2680.70	55.66	8.43	<LOD	<LOD	150.89	27.89	24482.23	535.08	24983.01	760.17	27.13	3.98	10970.22	2217.64	579.95	593.45	22.87	2.42	35.29	9.73	162.83	66.58	40.13	3.03	107.90	4.14	127924.16	1843.98	269.76	7.00	9.40	1.70	2286.79	150.90	95.47	52.29	118.79	7.78	305.56	72.20
Willshire-21	26.81	87.95	40251.03	1425.83	11.45	2.85	513.61	367.30	55203.82	2650.02	46.63	7.49	65.29	48.24	117.65	22.31	24305.14	531.08	25323.14	769.83	23.23	3.62	10723.44	2160.00	583.49	598.30	18.39	2.13	35.79	9.75	134.34	62.51	26.01	2.02	110.12	4.20	125704.62	1810.63	255.96	6.66	8.55	1.64	2250.62	149.74	108.68	55.79	94.32	6.05	300.56	71.03
Willshire-21	28.33	92.95	29893.82	1099.07	12.73	3.02	186.21	133.34	56702.87	2721.03	<LOD	<LOD	84.72	50.80	140.25	26.09	23333.51	508.52	23206.35	706.93	<LOD	<LOD	8700.36	1855.98	519.70	550.31	<LOD	<LOD	23.36	7.87	117.76	56.37	52.03	4.04	104.19	3.55	106603.60	1548.08	242.94	6.33	8.55	1.64	2234.30	148.26	101.74	53.58	99.05	6.49	406.11	95.92
Willshire-21	29.66	97.30	43879.69	1532.22	9.92	2.43	285.88	204.18	46245.04	2221.78	15.08	5.24	73.46	46.18	245.94	44.68	32828.32	711.48	29577.84	897.32	4.90	2.37	9074.12	1845.12	593.87	622.38	3.64	1.32	46.90	10.11	152.27	64.02	29.06	2.03	136.45	4.94	130732.50	1743.84	382.87	9.86	10.69	1.81	2649.98	177.23	134.66	65.10	145.77	9.02	223.60	52.80
Willshire-21	30.16	98.94	39872.24	1035.95	19.83	3.79	535.32	382.87	154076.28	7381.80	62.22	9.74	<LOD	<LOD	426.74	76.51	16689.23	372.68	11053.36	347.60	29.38	4.30	10780.86	4484.57	500.22	548.57	25.29	2.62	18.56	7.59	231.63	85.35	29.95	2.31	41.90	1.75	70249.12	1124.60	438.46	11.46	3.42	1.35	994.67	95.13	54.19	36.29	197.17	11.95	197.08	46.57
Willshire-21	31.08	101.97	21365.34	1000.76	28.00	5.89	272.48	194.52	121836.03	5837.05	30.27	6.53	54.13	34.68	419.43	75.24	22775.46	500.22	12158.84	379.53	13.90	2.96	21875.08	3602.38	598.44	603.15	11.13	1.72	51.78	10.37	<LOD	<LOD	40.79	3.36	45.61	1.85	89344.24	1354.27	225.89	5.90	4.27	1.39	1264.55	107.01	66.52	41.08	301.57	17.21	271.44	64.14
Willshire-21	42.15	138.28	13609.08	816.37	8.91	2.52	214.04	152.92	168459.68	8066.11	32.39	7.20	<LOD	<LOD	340.26	58.04	11459.25	260.77	8767.15	279.11	14.12	3.03	29270.91	4497.24	389.03	427.50	12.30	1.81	<LOD	<LOD	<LOD	<LOD	19.97	1.76	30.00	1.49	57236.18	945.41	156.20	4.16	1.94	1.48	616.47	72.50	41.67	29.13	136.93	8.61	65.78	15.61
Willshire-21	43.62	143.12	25187.60	1055.91	7.00	2.31	425.38	303.94	89785.17	4300.32	73.55	11.47	<LOD	<LOD	72.82	14.33	17120.78	379.00	14532.33	447.69	30.83	4.36	14583.28	2527.02	580.17	540.78	27.17	2.78	14.04	7.68	118.56	65.42	42.24	3.05	55.13	2.11	118196.83	1730.48	160.90	4.28	6.30	1.68	1734.03	121.91	67.52	39.77	76.65	5.38	301.24	71.17
Willshire-21	45.10	147.95	16384.87	818.83	5.73	2.20	311.06	222.47	112846.36	5403.60	58.45	9.62	<LOD	<LOD	191.47	33.39	11463.99	259.90	10543.48	328.22	26.24	3.93	23440.82	3603.47	<LOD	<LOD	22.00	2.39	<LOD	<LOD	<LOD	<LOD	21.12	1.82	41.25	1.75	79435.39	1222.71	146.02	3.92	3.39	1.53	1167.08	90.06	56.21	32.82	103.80	6.99	225.02	53.14
Willshire-21	46.62	152.95	30741.08	1192.03	12.73	3.02	416.06	297.38	75472.47	3615.96	59.86	9.51	<LOD	<LOD	98.15	18.58	18976.73	418.34	19414.21	591.73	27.44	4.18	13421.59	2568.49	557.02	541.61	22.78	2.47	21.68	7.76	171.98	77.42	16.90	1.61	75.43	2.69	122116.32	1775.62	219.43	5.74	10.90	2.21	2011.23	131.49	93.39	48.05	95.67	6.02	380.47	89.88
Willshire-21	48.14	157.95	24396.01	998.45	10.82	2.76	406.14	290.13	81807.14	3918.37	70.56	10.69	<LOD	<LOD	233.75	41.37	16333.11	362.41	14878.70	457.28	32.45	4.64	14683.89	2705.30	524.15	523.03	26.83	2.75	13.80	7.54	144.75	72.32	21.50	1.84	54.31	2.09	124880.05	1809.60	181.87	4.80	6.75	1.84	1894.20	123.52	66.43	40.28	93.36	5.93	565.95	133.64
Willshire-21	49.67	162.95	29239.52	1146.37	12.73	3.02	439.67	314.30	77457.86	3710.91	65.33	10.21	<LOD	<LOD	53.59	11.65	17961.93	396.81	18716.74	571.30	29.95	4.44	14340.08	2672.58	582.30	547.64	24.46	2.59	18.72	7.67	162.26	75.25	18.05	1.67	72.79	2.61	117451.17	1712.80	224.57	5.87	7.79	1.92	1848.09	124.02	79.91	44.09	106.86	6.96	372.63	88.03
Willshire-21	51.19	167.95	24971.06	1037.59	12.73	4.48	351.22	251.19	80404.95	3854.24	34.92	6.14	54.60	39.51	404.61	79.63	17265.37	382.17	17440.50	533.92	18.19	3.41	13898.92	2765.05	550.89	517.63	14.46	1.87	15.99	7.04	117.22	63.95	72.58	5.37	66.00	2.41	111340.35	1637.14	223.78	5.85	5.45	1.53	1701.82	119.23	84.09	44.29	194.56	11.52	341.81	80.76
Willshire-21	52.72	172.95	25960.51	1040.04	7.64	2.38	352.32	252.02	77989.10	3738.53	40.85	6.75	<LOD	<LOD	617.49	120.83	16411.25	363.90	16180.68	496.08	23.62	3.94	15770.91	2927.79	559.40	512.35	17.34	2.05	15.99	7.04	111.40	60.03	23.81	1.97	61.88	2.30	123163.77	1784.64	197.68	5.20	6.36	1.58	1814.06	122.12	72.03	40.80	175.61	10.28	378.79	89.48
Willshire-21	54.24	177.95	18198.78	813.84	9.55	2.59	301.44	215.11	88549.14	4243.40	37.22	6.23	<LOD	<LOD	1346.50	263.97	13581.92	303.92	11461.10	356.06	19.96	3.50	15367.09	2896.79	418.74	443.82	15.69	1.93	<LOD	<LOD	83.92	58.06	31.49	2.40	38.63	1.48	124764.02	1807.44	165.66	4.40	4.09	1.46	1745.83	116.70	55.41	35.68	161.41	9.63	676.90	159.82
Willshire-21	55.76	182.95	30237.37	1168.08	9.55	2.59	379.94	271.50	73016.26	3499.40	42.36	6.42	57.29	40.46	99.30	19.90	18960.00	417.91	19592.21	597.34	23.70	3.76	15049.75	3034.81	611.41	608.64	18.83	2.13	20.40	7.09	112.17	64.23	26.64	1.99	76.81	2.72	119347.82	1733.69	214.29	5.61	7.27	1.64	1881.12	126.76	96.42	49.98	95.50	6.10	372.40	87.97
Willshire-21	57.29	187.95	25981.13	1016.24	6.36	2.24	125.75	89.87	68021.28	3259.81	<LOD	<LOD	<LOD	<LOD	99.99	20.01	20664.90	452.20	19468.50	593.87	<LOD	<LOD	8436.60	546.38	555.36	<LOD	<LOD	18.13	7.03	95.53	61.97	51.12	3.87	80.17	2.82	115033.70	1608.55	217.85	5.70	7.72	1.68	2020.47	133.56	84.20	47.44	102.61	6.40	450.74	106.46
Willshire-21	58.81	192.95	32701.98	1228.54	8.91	2.52	360.86	258.05	68654.43	3291.06	35.69	5.95	56.19	40.10	108.21	21.38	19428.96	427.64	20354.62	620.49	19.41	3.38	15149.61	3015.47	578.90	591.49	15.18	1.91	21.76	7.13	141.67	67.23	28.44	2.09	78.31	2.77	127003.02	1832.19	206.38	5.41	6.81	1.63	1923.61	129.10	92.35	49.40	81.30	5.52	383.19	90.52
Willshire-21	60.34	197.95	33474.80	1263.45	8.91	2.52	421.50	301.27	68989.94	3305.90	55.67	8.01	<LOD	<LOD	52.93	11.02	19291.92	425.02	20226.40	616.14	28.76	4.28	15980.07	3131.47	660.54	671.63	23.64	2.44	20.17	7.51	<LOD	<LOD	35.26	2.39	78.98	2.78	126207.20	1825.93	204.46	5.36	8.18	1.71	2132.26	140.04	82.03	43.37	87.72	5.80	345.40	81.59
Willshire-21	61.86	202.95	30481.46	1163.98	12.73	3.02	409.22	292.44	69531.95	3331.32	53.05	7.71	43.80	32.82	421.07	67.63	19117.90	420.94	19874.37	605.35	27.98	4.21	13155.10	2724.98	647.19	670.56	22.82	2.40	23.53	7.62	103.47	64.73	16.41	1.45	77.87	2.75	123106.29	1782.18	212.71	5.57	7.72	1.68	2023.98	134.72	81.10	42.70	169.48	10.03	348.66	82.36
Willshire-21	63.43	208.12	31924.68	1210.83	7.64	2.37	393.47	281.75	66775.61	3199.93	46.48	7.16	<LOD	<LOD	69.58	13.14	19124.32	420.86	20064.18	611.49	24.31	3.89	13494.44	2774.29	620.98	648.36	19.51	2.18	26.89	7.73	140.35	70.17	17.11	1.48	78.98	2.78	124898.20	1808.22	206.82	5.42	7.72	1.68	2125.74	139.93	84.83	44.29	107.17	6.86	343.22	81.08
Willshire-21	64.91	212.95	33485.47	1248.29	11.20	3.09	431.66	308.39	67793.91	3249.70	53.01	7.94	45.37	34.60	107.78	18.05	20106.16	441.28	21302.91	648.11	28.69	4.36	13955.20	2820.45	626.05	599.05	23.55	2.49	22.86	7.54	175.29	77.35	41.89	3.30	82.96	2.90	122791.83	1776.69	208.69	5.46	8.72	1.87	2242.98	148.09	84.50	43.12	106.43	7.12	350.89	82.88
Willshire-21	66.43	217.95	27618.43	1084.35	11.20	3.09	454.82	325.58	73715.54	3532.59	57.33	8.39	71.02	36.59	40.56	8.16	19897.54	436.84	19253.31	587.73	30.73	4.59	12837.88	2704.39	554.13	559.26	25.04	2.61	29.05	8.21	158.51	75.02	23.04	1.75	74.48	2.65	121040.13	1755.31	197.03	5.17	6.78	1.72	1979.05	136.74	90.53	43.94	88.12	5.67	345.61	81.64
Willshire-21	67.96	222.95	28841.72	1086.24	10.50	2.98	382.61	273.46	65435.09	3136.22	47.48	7.33	<LOD	<LOD	46.36	9.22	18661.82	410.18	18805.84	573.55	24.91	3.99	12569.04	2567.32	654.21	604.64	19.11	2.17	19.05	7.41	98.49	64.64	16.76	1.46	75.22	2.67	122646.44	1767.43	202.47	5.31	7.75	1.79	2016.52	135.35	84.80	41.80	85.83	5.58	372.03	87.87
Willshire-21	69.48	227.95	31839.46	1203.89	7.64	4.08	397.12	283.84	66489.30	3186.76	41.48	6.42	52.75	41.20	97.25	19.55	19796.16	434.48	19407.69	591.74	22.43	3.56	17143.77	3603.26	652.72	577.88	16.86	2.02	23.57	7.20	175.76	72.99	133.00	8.36	77.37	2.73	124865.65	1804.29	196.76	5.16	7.27	1.75	2095.73	137.50	101.61	50.33	112.67	7.34	351.60	83.06
Willshire-21	71.00	232.95	43234.47	1525.64	9.55	2.59	474.19	338.85	57868.28	2775.78	42.93	6.61	76.49	50.80	1518.31	277.80	26157.36	569.85	28463.26	861.35	21.98	3.52	17825.72	3689.03	470.63	502.43	18.40	2.16	34.45	8.84	170.41	71.96	22.69	1.73	127.60	4.67	114380.35	1660.72	258.87	6.72	11.63	2.18	2425.39	160.62	135.81	63.18	398.34	21.46	225.99	53.37
Willshire-21	72.53	237.95	35619.44	1282.31	10.18	2.68	461.08	329.55	52570.64	2521.56	52.99	7.39	73.48	47.37	186.96	35.26	21090.54	461.94	20927.89	637.04	27.13	3.98	14617.90	3148.83	481.73	509.04	22.67	2.41	26.75	7.31	141.35	66.53	18.50	1.54	94.97	3.26	132215.85	1895.77	173.61	4.59	11.14	2.09	2681.05	166.50	100.63	52.20	108.88	7.19	293.46	69.29
Willshire-21	74.05	242.95	39867.41	1431.67	12.64	3.52	572.57	410.03	67.78	40.14	38.84	71.18	20.04	42.00	67.78	40.14	24365.75	531.73	25327.39	419.93	6.56	2.81	15200.22	2930.64	557.95	542.90	5.29	1.52	18.72	9.10	162.97	82.54	81.01	5.70	52.14	2.01	125740.61	1818.63	156.64	4.17	8.88	1.57	2499.31	158.64	88.20	51.19	197.85	11.74	1901.18	448.84
Willshire-21	75.58	247.95	26663.51	1066.03	18.08	4.65	238.70	170.67	79704.52	3820.07	19.13	5.63	70.82	43.46	145.37	24.98	24365.75	531.73	13527.39	419.93	6.56	2.81	15200.22	2930.64	557.95	542.90	5.29	1.52	18.72	9.10	162.97	82.54	81.01	5.70	52.14	2.01	125740.61	1818.63	156.64	4.17	8.88	1.57	2499.31	158.64	88.20	51.19	197.85	11.74	1901.18	448.84
Willshire-21	77.10	252.95	24091.47	977.89	14.58	3.45	427.67	305.80	78271.49	3750.91	53.67	8.27	50.25	37.88	108.11	19.07	22018.74	481.88	12636.55	392.28	27.16	4.27	12830.66	2599.41	597.63	560.74	21.23	2.39	20.20	9.13	<LOD	<LOD	46.08	3.72	51.78	2.00	123303.07	1784.79	157.41	4.19	8.07	1.52	2256.70	143.58	67.39	43.69	151.30	9.08	1279.00	301.96
Willshire-21	78.57	257.79	22559.98	911.21	16.33	3.27	161.10	115.20	60189.53	2884.71	8.69	4.57	44.56	37.40	112.35	20.83	23231.09	506.29	12493.89	387.19	<LOD	<LOD	10998.12	2320.98	709.71	596.35	<LOD	<LOD	17.97	8.04	138.72	73.11	43.56	3.48	53.53	2.05	138551.44	1982.90	155.87	4.15	10.26	1.77	2257.90	142.13	65.78	39.79	121.64	7.87	1557.17	367.62
Willshire-21	83.20	272.95	44753.54	1547.35	12.25	2.72	496.09	354.66	45899.17	2203.50	52.23	8.13	75.79	46.26	165.95	29.97	27686.62	602.26	27339.88	827.36	25.20	3.90	13114.43	2560.63	622.54	563.49	20.00	2.29	41.00	9.26	202.56	75.08	21.60	1.73	121.00	4.48	125084.90	1801.51	249.78	6.49	10.69	1.81	2414.51	156.98	117.71	55.01	125.95	8.05	248.70	58.73
Willshire-21	84.72	277.95	48896.33	1686.38	12.83	2.79	4032.90	158.31	42293.83	2032.77	45.94	7.93	83.16	64.02	99.44	18.79	32813.99	712.55	32391.45	979.26	20.94	3.82	11163.82	2382.89	1297.62	997.10	16.14	2.25	44.69	9.43	171.06	72.79	25.56	1.93	150.70	5.34	120589.36	1747.65	441.82	11.53	11.97	1.92	2638.44	198.55	139.11	70.20	132.23	8.31	202.91	47.93
Willshire-21	86.24	282.95	48945.76	1666.75	15.91	3.50	489.09	349.62	30065.49	1447.69	41.18	7.19	86.29	55.38	181.58	38.81

Portable X-Ray Fluorescence Data
Calculated elemental values are provided in terms of parts-per-million (ppm)
Elements Ag, Au, Bi, Cd, Cl, Co, Hf, Hg, Mo, Nb, Pd, Pr, Re, S, Sb, Se, Sn, Ta, U, W, and Y were consistently below the level of detection (<LOD) for both cores

Table A1-2. ***Domestic pXRF table showing calculated average elemental values and associated uncertainties with depth.***

Core	Depth (m)	Depth (ft)	Al	Al +/-	As	As +/-	Ba	Ba +/-	Ca	Ca +/-	Ce	Ce +/-	Cr	Cr +/-	Cu	Cu +/-	Fe	Fe +/-	K	K +/-	La	La +/-	Mg	Mg +/-	Mn	Mn +/-	Nd	Nd +/-	Ni	Ni +/-	P	P +/-	Pb	Pb +/-	Rb	Rb +/-	Si	Si +/-	Sr	Sr +/-	Th	Th +/-	Ti	Ti +/-	V	V +/-	Zn	Zn +/-	Zr	Zr +/-
Domestic	1.00	3.28	40543.19	1434.20	13.42	2.87	442.39	316.13	51309.59	2462.79	25.42	5.51	65.77	42.73	64.32	12.13	25223.07	549.49	28495.72	862.49	12.70	2.84	7324.20	1624.75	436.39	457.92	10.24	1.65	38.99	9.03	155.54	72.11	17.09	1.57	131.27	4.77	130609.40	1880.43	155.85	4.15	9.29	1.60	2173.31	149.42	127.09	59.70	96.83	6.07	230.72	54.49
Domestic	2.42	7.95	37934.87	1378.64	10.50	2.50	512.93	366.79	62890.57	3017.01	41.13	7.15	63.98	41.74	147.53	25.81	23876.70	522.17	27139.84	822.38	19.88	3.57	9395.66	1993.72	<LOD	<LOD	15.47	2.04	32.78	9.07	149.21	65.00	48.77	3.99	123.20	4.54	124036.25	1799.12	199.65	5.24	8.48	1.54	1994.25	139.25	124.46	59.31	100.36	6.83	221.42	52.30
Domestic	3.95	12.95	38015.00	1352.57	10.50	2.49	509.62	364.02	56528.12	2713.03	43.41	8.10	79.11	46.26	47.86	10.38	23655.05	516.73	27708.03	839.46	22.35	4.05	9419.60	2087.22	<LOD	<LOD	16.92	2.21	33.62	9.33	154.01	64.65	20.81	1.75	125.73	4.62	121975.99	1761.13	265.04	6.88	8.98	1.67	2033.87	140.25	129.39	59.22	85.36	5.54	248.46	58.68
Domestic	5.27	17.30	39941.40	1418.24	10.18	2.68	510.93	365.04	58087.29	2787.09	47.06	7.84	76.68	44.88	125.91	23.01	23345.61	509.82	28099.56	850.48	21.64	3.70	11605.26	2566.66	<LOD	<LOD	16.38	2.01	36.15	9.61	155.96	66.55	24.79	1.84	126.13	4.63	123318.41	1780.12	208.06	5.45	8.63	1.75	2021.72	139.93	118.34	54.11	92.33	5.90	217.07	51.28
Domestic	7.00	22.95	32819.35	1246.08	10.39	2.60	470.24	336.39	81698.09	3915.75	44.59	7.56	52.80	40.10	40.96	9.77	19872.30	436.54	21614.42	658.07	24.52	4.34	13793.05	2767.03	<LOD	<LOD	18.57	2.35	27.29	8.38	171.72	72.48	16.58	1.46	89.16	3.08	117558.58	1712.03	225.66	5.89	7.27	1.64	1803.82	127.73	84.43	45.30	94.66	6.36	234.68	55.42
Domestic	8.52	27.95	23196.65	979.39	9.92	2.43	548.67	392.29	98031.76	4695.07	64.39	9.38	<LOD	<LOD	76.09	17.04	15393.05	341.61	13640.12	421.03	35.52	5.52	15687.77	3113.18	<LOD	<LOD	29.54	3.20	<LOD	<LOD	140.46	67.88	26.09	1.85	49.41	1.94	119147.60	1735.44	223.07	5.82	4.70	1.40	1492.02	110.78	56.06	36.54	69.43	4.96	405.08	95.66
Domestic	10.04	32.95	36102.09	1355.19	8.17	2.23	529.77	378.64	77527.08	3714.04	50.89	8.14	52.56	35.02	76.09	17.74	21001.65	461.34	23395.29	709.30	28.15	4.70	15661.30	3316.31	<LOD	<LOD	20.69	2.38	34.83	10.15	162.04	69.46	20.88	1.70	97.52	3.52	120937.67	1761.32	321.75	8.31	6.41	1.50	1857.78	132.55	97.78	47.66	78.97	5.30	208.10	49.15
Domestic	11.57	37.95	33563.24	1288.12	8.91	2.52	469.00	335.13	77309.52	3703.39	43.92	7.38	51.02	38.81	167.51	30.72	20787.99	456.18	23029.30	699.42	23.85	4.17	12994.33	2812.57	<LOD	<LOD	18.16	2.28	27.03	8.38	164.36	73.24	35.67	2.56	95.13	3.27	118128.04	1727.82	356.27	9.18	7.69	1.58	1962.67	139.57	95.99	47.09	112.40	7.38	217.22	51.30
Domestic	13.09	42.95	35414.83	1324.39	11.90	3.19	469.42	335.39	75297.12	3607.72	40.16	6.96	52.28	32.59	78.44	16.02	21550.66	472.25	24302.65	736.84	21.95	3.89	13173.54	2798.55	<LOD	<LOD	17.55	2.27	29.09	9.57	156.19	69.58	19.08	1.61	101.73	3.94	118268.56	1722.30	334.10	8.62	6.46	1.41	1956.63	139.40	95.72	44.39	82.40	5.44	222.49	52.54
Domestic	14.62	47.95	37217.12	1374.19	10.18	2.68	485.84	347.44	73134.95	3504.83	44.40	7.13	42.10	33.08	321.67	65.49	20460.70	449.16	24140.50	731.34	22.72	3.82	13269.03	2722.29	<LOD	<LOD	18.96	2.22	28.81	8.71	164.16	73.81	23.74	1.78	103.19	3.98	119472.08	1737.67	429.89	11.23	6.41	1.49	1970.13	137.31	99.03	47.13	116.47	7.49	209.84	49.55
Domestic	16.14	52.95	37746.84	1401.95	10.23	2.28	425.90	304.58	72193.84	3462.84	35.49	7.00	<LOD	<LOD	125.33	24.29	20669.71	453.74	23927.32	726.61	18.75	3.90	13745.64	2901.31	<LOD	<LOD	12.82	1.90	30.29	8.91	196.07	80.84	13.61	1.34	104.50	3.87	121704.23	1772.16	368.70	9.50	6.78	1.72	1962.87	136.30	105.03	57.77	94.27	5.98	238.85	56.40
Domestic	17.66	57.95	36670.87	1345.13	10.23	2.28	491.10	351.14	70797.58	3396.95	43.00	7.43	46.37	41.58	49.59	10.41	20733.81	454.69	23988.63	729.06	24.67	4.46	14588.38	3154.37	<LOD	<LOD	18.16	2.30	33.79	9.63	146.89	63.80	17.28	1.53	105.60	4.06	117091.07	1701.90	372.68	9.60	7.27	1.65	1967.63	135.25	101.19	54.89	77.64	5.33	237.42	56.07
Domestic	18.89	61.97	34864.48	1338.56	9.92	2.43	500.42	357.93	80126.93	3841.78	52.77	8.48	63.32	40.24	179.43	34.12	20615.54	453.11	22913.83	696.18	25.59	4.26	16888.01	3868.08	<LOD	<LOD	22.29	2.63	23.70	8.67	172.78	74.32	15.61	1.50	93.44	3.22	117779.42	1721.78	344.13	8.87	6.84	1.52	1850.40	132.27	102.40	50.99	151.22	9.05	204.14	48.21
Domestic	20.61	67.62	35162.92	1305.45	10.18	2.68	530.19	379.15	74964.45	3592.87	56.12	8.93	53.93	42.15	86.75	18.98	22094.88	484.61	24109.75	731.48	26.08	4.26	14886.14	3252.59	465.96	528.77	22.06	2.52	35.15	10.26	158.99	71.05	24.15	1.92	103.13	4.03	116380.01	1690.79	357.34	9.21	7.72	1.68	2038.82	142.36	93.54	48.40	78.53	5.41	199.86	47.19
Domestic	22.34	73.28	31702.68	1220.78	7.64	2.37	478.93	342.48	86206.65	4130.47	45.22	7.55	53.13	40.50	41.67	10.09	18782.26	414.25	20782.64	632.49	23.48	3.94	14216.97	2927.20	<LOD	<LOD	17.52	2.17	22.87	8.22	136.47	64.67	15.12	1.44	82.41	2.89	112276.01	1641.83	367.13	9.46	5.45	1.53	1714.03	119.69	83.25	48.13	73.40	5.21	284.79	67.31
Domestic	23.66	77.62	36211.56	1376.36	10.18	2.68	573.59	410.26	85459.93	4096.84	65.65	9.82	60.16	39.24	266.68	46.90	20251.62	446.25	24234.10	735.61	30.76	4.81	14019.50	2883.70	<LOD	<LOD	25.19	2.71	27.12	9.18	180.27	73.66	15.12	1.44	98.63	3.89	115315.07	1690.19	443.19	11.57	8.18	1.71	1806.93	127.01	106.09	58.39	109.63	7.35	201.78	47.66
Domestic	25.18	82.62	42915.47	1523.08	21.64	4.42	562.45	402.13	54011.82	2592.10	52.58	8.55	72.22	43.54	162.72	29.24	24542.50	535.75	29010.41	877.85	25.65	4.43	10493.98	2277.99	375.90	419.97	19.69	2.19	38.40	9.30	181.09	71.67	15.71	1.42	135.28	4.88	125338.68	1812.23	413.73	10.83	9.54	1.82	2290.14	157.06	138.06	65.22	102.62	6.97	187.26	44.23
Domestic	27.11	88.94	33348.27	1278.92	7.64	2.37	497.64	355.50	74978.76	3592.39	59.24	8.94	54.96	39.11	164.18	30.15	20239.48	444.58	22055.96	670.05	30.54	4.67	14494.69	3146.24	391.98	435.80	22.99	2.36	37.46	9.06	130.06	68.67	34.56	2.35	90.07	3.10	124820.38	1813.93	322.13	8.32	6.84	1.52	1974.25	136.87	99.55	49.66	102.63	6.87	201.10	47.49
Domestic	27.93	91.64	29479.26	1205.61	9.55	2.60	507.72	362.75	97272.20	4658.65	53.36	7.91	32.30	30.70	48.77	9.78	15770.77	351.06	17768.01	542.88	27.72	4.07	21265.17	4045.39	<LOD	<LOD	22.65	2.38	15.91	7.65	169.10	74.84	13.01	1.40	67.48	2.45	112319.17	1656.46	319.82	8.26	5.56	1.44	1541.17	113.49	65.70	39.65	65.29	4.74	235.86	55.70
Domestic	29.86	97.95	29386.76	1148.40	7.00	2.11	485.06	346.62	72847.76	3496.49	51.20	7.89	49.00	33.34	47.64	9.51	17308.70	382.55	18454.30	562.52	25.57	3.84	12479.00	2445.77	365.05	401.65	21.57	2.30	12.71	8.08	135.24	69.05	12.63	1.38	68.60	2.48	124475.70	1805.72	297.78	7.70	6.36	1.58	1770.94	122.02	66.37	39.41	52.26	4.35	348.89	82.42
Domestic	31.38	102.95	26449.02	1084.26	4.67	1.92	502.53	359.19	90688.34	4345.58	59.54	8.65	39.00	31.33	107.50	18.98	15214.94	338.53	17153.63	524.81	28.65	4.11	15288.85	2844.58	<LOD	<LOD	24.98	2.53	15.36	8.15	142.33	70.64	30.10	2.24	62.86	2.31	113148.93	1659.67	397.95	10.44	5.45	1.53	1451.71	108.24	70.35	39.48	55.31	4.45	321.67	76.00
Domestic	32.90	107.95	28305.86	1147.82	4.67	1.92	499.26	357.00	91480.68	4383.91	59.20	8.76	39.00	31.03	98.34	17.61	14887.41	332.42	17545.49	536.00	28.48	4.09	18009.22	3190.88	<LOD	<LOD	24.34	2.50	10.59	8.04	168.88	72.78	17.47	1.59	62.66	2.31	116039.11	1699.50	398.33	10.45	5.90	1.55	1537.64	111.18	60.39	37.46	52.64	4.36	248.89	58.80
Domestic	34.23	112.30	21972.38	994.54	6.42	2.06	492.63	352.41	118857.60	5695.15	66.53	9.62	<LOD	<LOD	32.49	8.83	11570.82	262.95	13711.72	422.47	32.71	4.66	24939.67	4144.61	<LOD	<LOD	27.62	2.72	<LOD	<LOD	110.44	71.80	10.80	1.28	46.35	1.87	92958.83	1402.16	414.50	10.86	2.99	1.34	1215.59	95.23	45.55	31.55	50.43	4.35	208.00	49.13
Domestic	35.85	117.62	33858.32	1250.94	18.67	3.61	516.85	369.58	60187.07	2887.65	55.88	8.41	65.09	41.49	43.79	10.41	22147.18	485.91	20804.03	634.55	28.00	4.13	13588.06	2537.50	<LOD	<LOD	23.20	2.38	28.86	8.53	156.95	71.98	17.28	1.53	91.96	3.17	135577.62	1946.97	463.20	12.08	7.27	1.55	2133.86	144.61	91.10	47.47	77.20	5.29	234.00	55.26
Domestic	37.78	123.94	35061.07	1342.03	5.83	2.01	576.73	412.37	89068.80	4269.53	57.74	8.80	55.54	39.93	57.21	13.28	20308.63	448.19	25400.57	770.29	27.54	4.16	16116.46	2980.66	<LOD	<LOD	22.39	2.37	31.48	9.62	203.18	83.42	15.12	1.44	104.93	4.06	108074.53	1592.67	404.37	10.60	7.69	1.58	1816.65	131.57	90.13	47.02	68.28	4.96	153.74	36.33
Domestic	39.10	128.28	30834.91	1235.82	8.17	2.23	525.36	375.44	99073.22	4746.70	56.11	8.18	<LOD	<LOD	33.56	8.71	16265.47	361.42	20819.48	633.86	30.19	4.50	17609.46	3580.24	<LOD	<LOD	24.08	2.47	16.81	7.42	153.66	71.40	13.32	1.37	77.56	2.75	108838.36	1608.26	329.50	8.50	5.13	1.42	1558.64	117.04	65.19	38.38	54.93	4.54	176.65	41.73
Domestic	40.62	133.28	29744.58	1206.92	4.67	1.92	548.78	392.42	101345.33	4855.72	60.96	8.68	40.85	29.81	34.24	8.78	15351.03	342.45	19725.89	601.82	32.29	4.73	20754.96	4003.31	<LOD	<LOD	26.55	2.64	14.89	7.37	185.00	75.26	14.40	1.41	71.97	2.58	108023.27	1596.74	311.71	8.05	5.56	1.44	1503.16	115.61	68.95	39.10	54.54	4.52	190.81	45.06
Domestic	42.15	138.28	33769.39	1294.71	4.67	1.92	523.48	374.36	87846.81	4209.38	57.43	8.37	46.40	31.42	40.41	9.62	19129.93	421.92	23647.23	717.42	29.65	4.49	16015.62	3301.99	<LOD	<LOD	23.53	2.46	22.57	7.58	177.10	73.96	14.76	1.42	92.10	3.18	113778.33	1665.31	344.58	8.89	5.98	1.47	1793.56	128.67	79.29	42.37	74.55	5.23	175.60	41.48
Domestic	43.67	143.28	26874.45	1139.33	5.25	1.96	564.51	403.60	112507.98	5389.58	61.39	8.21	37.42	31.33	54.62	11.47	13174.51	296.21	16770.62	515.26	33.55	4.64	20286.33	3844.34	<LOD	<LOD	28.12	2.71	<LOD	<LOD	207.50	79.60	11.88	1.31	56.63	2.15	103840.20	1545.54	302.46	7.82	3.85	1.36	1282.08	102.40	53.30	37.46	62.28	4.85	248.80	58.79
Domestic	45.20	148.28	24829.75	1086.48	4.08	1.89	539.71	385.51	118515.86	5676.96	60.46	8.14	<LOD	<LOD	37.67	8.47	12028.24	272.06	15614.15	479.64	32.18	4.48	22405.64	4142.94	<LOD	<LOD	27.89	2.69	<LOD	<LOD	161.95	73.96	11.52	1.30	53.25	2.06	99651.33	1492.30	295.90	7.65	3.42	1.35	1139.45	93.44	43.46	33.75	51.50	4.49	178.69	42.20
Domestic	46.72	153.28	26381.38	1117.54	3.50	1.86	526.77	376.60	114880.16	5502.83	57.24	7.87	<LOD	<LOD	16.32	6.31	13165.41	296.20	17241.22	527.04	30.02	4.29	21530.21	3988.29	<LOD	<LOD	26.05	2.56	<LOD	<LOD	137.41	68.38	11.88	1.31	59.63	2.23	99147.89	1481.55	317.51	8.20	4.27	1.38	1326.73	100.81	49.23	35.63	54.69	4.59	189.89	44.84
Domestic	48.24	158.28	21885.11	982.56	4.90	2.33	549.40	392.72	116536.80	5579.22	69.40	10.23	<LOD	<LOD	45.20	10.62	11360.51	257.28	14206.26	436.18	35.91	5.33	20837.32	4064.06	<LOD	<LOD	30.05	3.06	<LOD	<LOD	111.91	61.34	10.16	1.18	44.98	1.83	101795.93	1518.68	289.84	7.50	3.63	1.44	1238.41	93.24	38.40	29.57	53.45	3.85	280.18	66.17
Domestic	49.57	162.62	28963.15	1162.77	6.30	2.46	507.81	362.94	99118.05	4745.88	65.93	9.88	42.65	33.19	130.66	26.00	15692.84	349.16	18916.61	576.11	33.88	5.20	14522.92	2824.09	<LOD	<LOD	27.52	2.89	11.98	7.02	142.46	65.72	11.86	1.23	66.74	2.42	113221.57	1660.80	351.00	9.05	5.45	1.53	1523.13	109.33	59.17	35.59	56.59	4.45	255.84	60.42
Domestic	51.29	168.28	19551.65	891.84	4.20	2.27	513.60	367.35	111856.43	5354.36	73.11	10.61	<LOD	<LOD	14.13	6.93	11304.85	256.29	12428.08	383.15	37.18	5.46	17368.82	3186.26	<LOD	<LOD	31.95	3.20	<LOD	<LOD	129.52	62.77	10.50	1.19	38.72	1.67	109013.60	1607.35	276.59	7.17	1.82	1.38	1177.43	89.24	36.19	28.36	52.44	4.32	394.75	93.26
Domestic	53.12	174.27	29501.33	1177.53	5.25	1.96	505.45	361.52	94526.63	4528.41	62.31	9.49	42.81	35.42	40.26	9.89	17022.18	377.45	20742.80	630.84	31.60	4.79	14458.76	2826.80	402.45	462.65	25.72	2.69	<LOD	<LOD	177.21	75.61	16.72	1.55	76.07	2.70	112686.30	1654.06	373.23	9.62	5.13	1.42	1688.28	118.56	70.98	42.35	53.54	4.45	239.72	56.62
Domestic	54.24	177.95	16862.15	793.07	4.08	1.89	541.63	386.97	109613.43	5249.37	70.89	10.28	<LOD	<LOD	8.48	6.56	10694.11	243.99	11019.42	341.83	36.38	5.30	18227.02	3251.35	<LOD	<LOD	29.43	2.95	<LOD	<LOD	103.68	62.42	9.66	1.28	34.68	1.58	105844.50	1560.92	276.76	7.18	2.56	1.32	1335.04	96.49	35.99	30.38	36.85	3.98	367.94	86.93
Domestic	55.86	183.28	19113.30	880.14	4.67	1.94	545.22	389.46	115797.49	5545.39	73.16	10.57	59.87	32.82	81.22	17.48	13248.46	297.98	11864.08	367.79	38.06	5.50	19612.66	3482.76	427.97	480.63	31.34	3.11	<LOD	<LOD	155.26	72.91	13.38	1.41	36.54	1.63	106330.75	1569.52	279.13	7.24	<LOD	<LOD	1174.54	91.71	39.02	31.46	85.74	5.63	642.84	151.80
Domestic	57.39	188.28	23586.65	1012.95	4.08	1.89	498.24	355.89	102639.38	4917.12	59.22	8.59	43.89	33.91	23.31	7.73	12736.27	286.88	15438.08	473.11	28.88	4.05	20301.33	4008.88	<LOD	<LOD	25.63	2.60	<LOD	<LOD	205.18	86.72	11.52	1.34	52.95	2.05	107544.87	1588.34	305.32	7.90	4.04	1.30	1387.55	100.67	55.60	36.63	49.33	4.38	284.23	67.12
Domestic	58.91	193.28	18845.00	878.64	3.50	1.85	558.78	399.80	115974.22	5555.33	68.78	9.46	52.74	35.18	17.66	7.18	12351.99	279.42	11556.11	359.36	33.61	4.49	21538.05	4223.06	<LOD	<LOD	30.82	2.96	<LOD	<LOD	259.34	97.47	18.95	1.66	36.17	1.62	102809.24	1527.25	268.43	6.97	3.63	1.28	1278.82	97.55	46.05	34.51	53.28	4.50	603.91	142.61
Domestic	60.44	198.28	18559.31	898.09	8.75	2.30	283.83	203.13	127997.59	6130.39	22.22	5.60	<LOD	<LOD	248.60	47.94	21849.20	481.02	11392.67	356.54	11.66	2.78	28698.46	5357.17	480.98	498.05	9.95	1.69	<LOD	<LOD	153.02	85.19	21.55	1.79	35.80	1.61	83542.19	1270.64	253.13	6.58	4.44	1.31	1953.23	134.01	71.97	46.46	172.46	10.74	1688.82	398.75
Domestic	62.06	203.61	18842.55	886.31	5.83	2.01	461.11	329.60	116725.88	5589.07	45.33	6.71	<LOD	<LOD	63.56	14.66	12872.17	289.09	12151.57	377.03	23.12	3.57	21554.83	4170.86	<LOD	<LOD	20.14	2.23	<LOD	<LOD	210.43	89.75	15.40	1.45	39.45	1.69	101502.43	1511.05	269.82	7.00	3.85	1.36	1120.43	89.75	42.61	32.46	54.54	4.52	480.94	113.59
Domestic	63.18	207.30	19849.56	955.78	8.75	2.29	368.68	263.52	131886.59	6315.58	35.79	6.12	<LOD	<LOD	83.34	17.82	14067.61	315.34	13891.00	428.43	19.55	3.39	26999.77	5059.11	<LOD	<LOD	16.14	2.01	<LOD	<LOD	<LOD	<LOD	14.40	1.41	48.30	1.91	77689.61	1205.19	296.18	7.66	2.99	1.33	1025.54	87.25	55.83	35.10	110.26	7.40	269.33	63.63
Domestic	65.01	213.28	19206.02	884.65	8.75	2.29	458.14	319.19	123611.16	5757.66	57.62	7.88	<LOD	<LOD	180.80	35.43	12912.68	284.75	13116.52	399.45	31.50	4.41	25008.08	4703.27	<LOD	<LOD	27.18	2.74	<LOD	<LOD	73.21	64.15	18.36	1.58	54.25	1.81	78678.30	1220.92	232.27	6.05	3.42	1.35	1051.74	82.80	55.83	34.83	65.15	5.65	238.43	56.31
Domestic	66.23	217.30	19841.40	915.78	5.83	2.01	546.17	390.49	117349.31	5620.23	71.71	10.40	54.69	31.48	29.51	7.53	14410.49	322.93	11906.21	369.23	37.15	5.55	20791.20	3625.44	425.31	468.41	30.93	3.14	<LOD	<LOD	233.99	83.39	16.72	1.55	36.34	1.62	104172.88	1543.67	254.00	6.60	2.42	1.25	1532.33	112.08	44.62	32.36	62.64	4.88	636.23	150.22
Domestic	68.26	223.94	20116.44	982.55	11.67	2.64	406.13	290.28	133790.55	6409.62	57.42	8.95	<LOD	<LOD	62.15	12.84	12508.70	283.14	13081.05	405.20	31.36	4.93	25447.34	4360.26	<LOD	<LOD	24.84	2.68	<LOD	<LOD	109.29	69.34	15.61	1.51	44.87	1.83	81652.77	1263.82	295.29	7.64	2.42	1.25	956.87	88.17	65.22	34.69	84.33	5.71	162.50	38.39
Domestic	69.58	228.28	14297.64	816.23	7.58	2.17	390.76	279.36	157736.69	7554.85	62.14	9.47	<LOD	<LOD	168.24	29.68	9867.49	227.62	10899.95	340.78	32.50	5.08	26258.47	4511.28	<LOD	<LOD	27.05	2.86	<LOD	<LOD	<LOD	<LOD	27.50	2.10	34.48	1.57	66382.58	1065.41	249.32	6.48	<LOD	<LOD	710.84	76.53	43.69	28.64	65.86	4.99	103.56	24.50
Domestic	92.34	302.95	24741.07	950.14	9.33	2.36	457.25	326.80	51949.58	2491.48	57.98	8.11	51.10	35.02	51.66	10.63	16791.22	371.00	14987.47	459.93	28.93	4.12	10418.78	2187.46	930.69	739.50	24.32	2.46	14.83	8.14	90.64	55.28	21.12	1.82	56.36	2.13	150648.83	2140.46	130.51	3.54	6.06	1.39	2119.10	140.16	68.92	41.22	115.50	7.45	442.20	104.41
Domestic	93.86	307.95	28481.54	1052.85	9.92	2.43	452.59	323.50	43310.40	2078.29	52.93	7.67	68.02	38.88	28.41	7.60	18939.89	416.50	17639.72	537.69	27.73	3.98	10078.59	2125.56	865.60	703.98	22.37	2.34	21.18	8.31	135.77	58.73	19.58	1.74	73.79	2.63	152936.53	2169.84	148.81	3.98	7.27	1.46	2488.06	158.86	85.90	46.28	105.58	6.56	378.46	89.38
Domestic	95.39	312.95	46720.33	1580.15	10.50	2.50	558.25	399.08	25648.34	1237.18	48.20	7.41	92.88	51.96	36.81	8.61	31840.91	690.93	31009.18	937.77	23.02	3.66	8757.25	1973.11	702.86	625.95	18.30	2.11	48.72	11.05	110.38	56.48	25.73	2.07	156.10	5.51	132284.80	1892.11	269.97	7.00	10.90	1.72	2958.94	195.61	160.93	73.83	120.27	7.

Table A2-1. ***Willshire-21 particle size analysis table showing grain size as a percentage with depth.***

Willshire-21 particle size data		>2000 µm	63-2000 µm	2-63 µm	<2 µm	32-64 mm	16-32 mm	8-16 mm	4-8 mm	2-4 mm	1-2 mm	0.5-1 mm	0.25-0.5 mm	0.125-0.25 mm	0.063-0.125 mm	0.032-0.063 mm	0.016-0.032 mm	0.008-0.016 mm	0.004-0.008 mm	0.002-0.004 mm	<0.002 mm	
Depth (m)	Depth (ft)	% GRAVEL	% SAND	% SILT	% CLAY	% VERY COARSE GRAVEL	% COARSE GRAVEL	% MEDIUM GRAVEL	% FINE GRAVEL	% VERY FINE GRAVEL	% VERY COARSE SAND	% COARSE SAND	% MEDIUM SAND	% FINE SAND	% VERY FINE SAND	% VERY COARSE SILT	% COARSE SILT	% MEDIUM SILT	% FINE SILT	% VERY FINE SILT	% CLAY	Method
0.60	1.97		10.14	74.69	15.17						0.00	1.04	2.11	2.72	4.27	7.96	12.61	18.18	20.19	15.77	15.17	laser diffraction
2.72	8.94		16.36	63.07	19.97						2.24	3.40	2.99	3.46	4.27	5.92	9.09	14.46	17.63	15.96	19.97	laser diffraction
3.95	12.95		14.74	64.94	19.85						1.76	2.77	2.68	3.28	4.25	6.00	9.27	14.84	18.32	16.51	19.85	laser diffraction
4.87	15.98		14.69	65.92	19.36						0.87	2.83	3.01	3.54	4.43	6.14	9.53	15.17	18.57	16.52	19.36	laser diffraction
6.40	20.98		12.31	67.42	20.26						0.33	1.86	2.37	3.23	4.52	6.16	9.46	15.37	19.16	17.28	20.26	laser diffraction
7.92	25.98		14.32	65.52	19.98						1.13	3.03	3.13	3.00	4.03	5.88	9.16	14.91	18.65	16.92	19.98	laser diffraction
10.34	33.94		29.40	61.64	8.95						0.00	2.15	4.43	7.92	14.90	17.05	15.00	12.56	9.59	7.43	8.95	laser diffraction
10.97	35.98		32.69	56.80	10.52						0.00	2.96	8.69	11.01	10.03	10.41	11.64	13.29	12.32	9.14	10.52	laser diffraction
12.49	40.98		11.95	73.28	14.78						0.12	1.56	1.99	2.61	5.66	10.83	14.94	18.11	16.86	12.54	14.78	laser diffraction
14.02	45.98		5.29	76.88	17.83						0.02	0.80	0.73	0.84	2.90	9.40	16.01	18.68	18.01	14.77	17.83	laser diffraction
15.54	50.98		4.03	76.30	19.67						0.38	1.20	0.51	0.37	1.58	6.39	15.14	19.85	19.10	15.82	19.67	laser diffraction
17.06	55.98		2.88	77.74	19.38						0.43	1.22	0.39	0.00	0.84	6.75	15.78	19.95	19.17	16.09	19.38	laser diffraction
18.54	60.82		35.19	52.64	12.16						0.83	8.05	10.16	8.42	7.73	10.00	12.38	12.23	9.85	8.19	12.16	laser diffraction
20.11	65.98		31.26	56.01	12.73						0.24	5.60	9.70	8.20	7.51	9.69	12.66	13.18	11.30	9.17	12.73	laser diffraction
22.54	73.94		32.90	54.52	12.59						0.03	3.48	9.53	10.81	9.05	9.52	10.86	11.76	11.92	10.45	12.59	laser diffraction
23.16	75.98		32.96	53.71	13.33						0.11	4.42	9.32	10.38	8.74	9.29	10.82	11.83	11.68	10.09	13.33	laser diffraction
25.58	83.94		18.99	67.31	13.70						0.29	2.76	3.77	6.07	6.11	6.82	10.12	16.05	19.20	15.11	13.70	laser diffraction
27.11	88.94		18.87	67.46	13.67						0.03	1.78	3.64	6.71	6.71	7.35	10.36	15.76	18.95	15.05	13.67	laser diffraction
27.73	90.98		16.59	71.56	11.85						0.00	1.44	3.48	5.82	5.85	7.42	12.10	18.12	19.54	14.39	11.85	laser diffraction
29.26	95.98		6.81	78.20	14.99						0.32	1.65	0.96	1.21	2.67	5.68	11.92	20.41	22.97	17.22	14.99	laser diffraction
30.78	100.98	71.20	28.20	0.60		14.40	27.20	11.70	9.10	8.90	7.50	10.20	6.40	3.30	0.60			0.60				sieve
32.55	106.80	66.50	31.80	1.70		6.90	27.00	12.70	9.50	10.30	11.50	9.40	4.00	4.80	2.10			1.70				sieve
33.78	110.82	62.50	35.70	1.80			2.60	16.50	27.20	16.10	11.10	10.50	6.10	5.40	2.70			1.80				sieve
35.50	116.48	21.40	74.20	4.30			4.70	5.00	6.10	5.60	7.90	21.20	20.10	16.30	8.70			4.30				sieve
37.03	121.48	44.40	54.50	1.10			21.90	6.50	5.50	10.40	24.30	22.70	4.30	2.10	1.30			1.10				sieve
38.45	126.15	54.30	44.70	1.00			5.10	12.70	15.90	20.50	25.20	13.50	3.30	1.50	1.20			1.00				sieve
39.97	131.15	79.60	19.40	1.00		13.60	33.00	14.90	9.20	8.80	7.40	6.20	2.70	1.70	1.40			1.00				sieve
42.25	138.61		29.99	54.48	15.53						0.34	6.14	7.36	6.90	9.26	11.37	11.50	11.83	10.59	9.19	15.53	laser diffraction
43.45	142.54		30.16	62.91	6.93						0.45	3.50	6.06	9.50	10.65	12.95	15.49	15.72	11.53	7.22	6.93	laser diffraction
44.60	146.31		31.45	57.00	11.55						0.06	3.29	7.42	10.64	10.05	10.81	11.91	12.98	11.93	9.37	11.55	laser diffraction
46.05	151.07		28.48	61.31	10.22						0.00	2.52	7.50	9.71	8.74	9.38	11.47	14.34	14.87	11.25	10.22	laser diffraction
47.57	156.07		29.07	61.11	9.82						0.11	3.56	7.32	9.46	8.62	9.27	11.45	14.39	14.87	11.14	9.82	laser diffraction
49.09	161.07		40.97	50.77	8.23						1.62	5.60	9.15	13.07	11.53	10.61	10.08	10.92	10.89	8.27	8.23	laser diffraction
50.62	166.07		34.37	53.13	12.50						0.08	3.75	8.76	11.64	10.15	10.15	10.61	11.43	11.38	9.56	12.50	laser diffraction
52.14	171.07		21.06	67.91	11.03						0.00	0.89	4.43	7.24	8.49	10.40	12.84	16.88	16.64	11.15	11.03	laser diffraction
54.54	178.94		24.39	64.62	10.98						0.06	2.15	5.40	8.63	8.15	9.55	12.51	16.40	15.69	10.47	10.98	laser diffraction
55.16	180.98		33.47	55.73	10.80						0.05	3.42	8.51	11.23	10.24	10.50	11.26	12.50	12.16	9.31	10.80	laser diffraction
56.69	185.98		32.39	57.44	10.18						0.04	2.70	7.90	10.95	10.80	11.88	12.42	12.57	11.68	8.90	10.18	laser diffraction
58.21	190.98		33.02	56.19	10.79						0.20	3.61	7.30	11.22	10.68	11.31	11.86	12.25	11.67	9.10	10.79	laser diffraction
59.74	195.98		33.45	56.50	10.05						0.46	4.66	7.59	10.43	10.31	11.60	12.26	12.35	11.52	8.76	10.05	laser diffraction
61.26	200.98		31.51	59.86	8.63						0.00	1.45	5.05	9.33	15.69	17.67	14.08	11.55	9.46	7.10	8.63	laser diffraction
62.78	205.98		32.97	56.35	10.68						0.00	2.52	7.89	11.44	11.12	11.54	12.03	12.44	11.45	8.89	10.68	laser diffraction
64.31	210.98		33.78	56.10	10.13						0.21	2.91	7.69	11.62	11.35	11.87	12.13	12.29	11.14	8.68	10.13	laser diffraction
65.83	215.98		34.65	55.24	10.11						0.70	4.58	7.32	11.19	10.86	11.41	12.05	12.28	11.03	8.47	10.11	laser diffraction
67.36	220.98		29.37	60.59	10.04						0.19	3.75	7.37	9.51	8.55	9.43	11.70	14.38	14.25	10.83	10.04	laser diffraction
68.88	225.98		41.96	49.40	8.64						0.33	6.18	13.88	13.75	7.82	8.18	9.51	11.24	11.45	9.02	8.64	laser diffraction
70.55	231.48		2.79	80.80	16.17						0.96	1.17	0.33	0.00	0.33	2.63	11.30	23.26	25.19	18.41	16.17	laser diffraction
71.93	235.98		3.29	80.24	16.14						1.22	1.57	0.50	0.00	0.00	0.89	7.35	22.71	29.31	19.99	16.14	laser diffraction
73.90	242.46		2.07	87.56	10.37						0.00	0.00	0.00	0.01	2.06	11.64	22.59	24.91	17.64	10.79	10.37	laser diffraction
74.98	245.98		53.57	43.93	2.50						0.00	0.00	1.01	16.77	35.80	26.55	8.37	4.06	2.84	2.11	2.50	laser diffraction
76.40	250.66		83.53	15.27	1.20						0.00	0.00	5.01	45.43	33.09	6.53	3.64	2.14	1.70	1.26	1.20	laser diffraction
78.02	255.98		77.65	20.42	1.93						0.00	0.00	2.83	34.43	40.39	8.50	3.93	3.30	2.63	2.05	1.93	laser diffraction
79.60	261.15	88.50	10.50	1.00		17.60	20.90	21.90	17.10	11.00	3.30	2.20	1.40	2.10	1.40			1.00				sieve
81.12	266.15	89.10	10.30	0.60		17.20	24.40	19.60	18.90	8.90	3.80	2.30	1.30	1.30	1.50			0.60				sieve
83.05	272.46		9.16	71.18	19.45						1.16	2.12	1.51	1.68	2.70	5.90	10.22	16.51	20.72	17.82	19.45	laser diffraction
84.12	275.98		3.70	83.11	13.19						0.00	0.72	0.30	0.01	2.67	11.22	15.91	19.64	20.95	15.38	13.19	laser diffraction
85.64	280.98		2.73	81.42	15.84						0.55	1.30	0.37	0.00	0.52	7.77	13.96	18.46	23.10	18.13	15.84	laser diffraction
87.17	285.98		5.00	75.59	18.71						2.03	2.09	0.51	0.00	0.37	2.02	8.52	19.16	25.17	20.72	18.71	laser diffraction
88.69	290.98		1.35	86.04	12.61						0.02	0.71	0.19	0.01	0.43	2.27	14.59	28.38	25.56	15.23	12.61	laser diffraction
90.22	295.98		22.47	65.20	12.33						0.26	3.99	5.53	5.70	6.99	10.48	13.13	15.68	14.82	11.09	12.33	laser diffraction
91.74	300.98		24.60	61.80	13.60						0.08	3.63	6.47	7.17	7.25	8.57	10.44	14.15	15.86	12.78	13.6	laser diffraction
93.26	305.98		15.81	70.70	13.49						0.17	2.14	3.54	4.69	5.26	6.76	11.12	17.79	19.87	15.16	13.49	laser diffraction
95.69	313.94		14.18	72.28	13.55						0.00	1.00	3.19	3.96	6.02	8.36	11.61	17.84	19.79	14.67	13.55	laser diffraction
96.31	315.98		10.38	73.48	16.14						0.11	1.09	1.35	2.77	5.05	7.22	10.91	18.06	20.79	16.49	16.14	laser diffraction
97.89	321.15	71.9	26.2	1.80			6.70	25.90	22.30	17.10	9.20	6.00	4.70	3.60	2.60			1.80				sieve
99.69	327.05		3.40	81.70	14.78						0.76	1.16	0.30	0.009	1.16	4.12	10.84	22.99	25.96	17.8	14.78	laser diffraction

Table A2-2. ***Domestic particle size analysis table showing grain size as a percentage with depth.***

Domestic particle size data		>2000 µm	63-2000 µm	2-63 µm	<2 µm	32-64 mm	16-32 mm	8-16 mm	4-8 mm	2-4 mm	1-2 mm	0.5-1 mm	0.25-0.5 mm	0.125-0.25 mm	0.063-0.125 mm	0.032-0.063 mm	0.016-0.032 mm	0.008-0.016 mm	0.004-0.008 mm	0.002-0.004 mm	<0.002 mm	
Depth (m)	Depth (ft)	% GRAVEL	% SAND	% SILT	% CLAY	% VERY COARSE GRAVEL	% COARSE GRAVEL	% MEDIUM GRAVEL	% FINE GRAVEL	% VERY FINE GRAVEL	% VERY COARSE SAND	% COARSE SAND	% MEDIUM SAND	% FINE SAND	% VERY FINE SAND	% VERY COARSE SILT	% COARSE SILT	% MEDIUM SILT	% FINE SILT	% VERY FINE SILT	% CLAY	Method
1.20	3.94	0.00	14.53	63.56	21.44						1.71	2.67	2.76	3.29	4.10	5.91	8.68	14.14	17.80	17.03	21.44	laser diffraction
2.82	9.27	0.00	16.03	61.69	21.49						2.42	2.86	2.33	3.38	5.04	6.76	8.53	13.15	16.86	16.40	21.49	laser diffraction
4.25	13.94	0.00	14.27	62.26	22.75						2.26	2.93	2.50	2.93	3.65	5.16	7.91	13.73	17.99	17.46	22.75	laser diffraction
5.57	18.28	0.00	10.17	64.90	24.39						1.76	2.10	1.76	2.09	2.46	4.00	7.66	14.15	19.35	19.74	24.39	laser diffraction
7.40	24.27	0.00	21.78	62.84	15.37						0.02	2.31	5.12	6.74	7.59	9.08	11.05	14.39	15.33	12.99	15.37	laser diffraction
8.22	26.97	0.00	15.43	74.32	10.25						0.00	0.00	0.39	4.67	10.37	12.35	16.22	19.86	15.95	9.94	10.25	laser diffraction
10.34	33.94	0.00	20.10	62.35	17.55						0.73	3.57	4.16	5.38	6.27	7.89	9.90	13.94	16.22	14.40	17.55	laser diffraction
11.87	38.94	0.00	16.69	64.71	18.60						0.13	2.13	3.52	4.95	5.95	7.69	10.03	14.55	17.17	15.28	18.60	laser diffraction
13.39	43.94	0.00	17.93	64.29	17.78						0.28	2.71	3.74	4.96	6.25	8.10	10.34	14.45	16.69	14.70	17.78	laser diffraction
14.92	48.94	0.00	16.61	65.55	17.84						0.57	2.83	3.06	4.13	6.01	8.35	10.94	14.95	16.73	14.58	17.84	laser diffraction
16.44	53.94	0.00	15.73	66.69	17.59						0.00	1.15	3.57	4.71	6.29	8.75	11.34	15.20	16.88	14.53	17.59	laser diffraction
17.96	58.94	0.00	19.48	64.02	16.50						0.19	2.42	4.49	5.65	6.73	8.93	11.28	14.37	15.80	13.64	16.50	laser diffraction
19.09	62.62	0.00	18.06	64.18	17.76						0.35	2.65	3.87	4.99	6.18	8.16	10.47	14.34	16.65	14.56	17.76	laser diffraction
20.91	68.61	0.00	21.93	60.98	17.10						1.03	4.37	4.74	5.80	5.99	7.20	9.40	13.63	16.37	14.38	17.10	laser diffraction
22.54	73.94	0.00	17.74	64.96	17.30						0.09	2.37	3.96	4.92	6.41	9.09	11.76	14.65	15.70	13.77	17.30	laser diffraction
24.06	78.94	0.00	13.21	65.80	20.88						0.82	2.19	2.36	3.19	4.64	6.92	10.23	14.60	17.61	16.43	20.88	laser diffraction
25.38	83.28	0.00	90.75	8.10	1.15						0.00	2.41	31.30	43.89	13.15	2.72	1.67	1.34	1.30	1.08	1.15	laser diffraction
27.21	89.27	0.00	26.96	59.59	13.45						1.08	6.73	7.30	5.88	5.97	7.99	11.29	14.64	14.31	11.36	13.45	laser diffraction
28.53	93.61	0.00	37.14	51.00	11.86						0.00	3.24	10.75	12.20	10.94	10.22	9.98	10.84	10.78	9.19	11.86	laser diffraction
30.16	98.94	0.00	43.17	45.97	10.85						0.00	3.91	13.48	15.26	10.51	9.53	9.28	9.73	9.45	7.98	10.85	laser diffraction
31.78	104.27	0.00	41.92	47.39	10.68						0.02	3.35	12.83	14.83	10.90	10.14	9.89	9.99	9.44	7.93	10.68	laser diffraction
33.30	109.27	0.00	56.66	37.77	5.57						0.00	0.84	3.90	17.07	34.85	17.39	6.27	5.72	4.47	3.90	5.57	laser diffraction
34.83	114.27	0.00	20.83	66.87	12.30						0.00	1.75	4.07	6.13	8.88	12.37	15.45	15.92	13.27	9.87	12.30	laser diffraction
36.15	118.61	0.00	25.10	64.03	10.87						0.03	2.15	5.21	7.61	10.10	12.64	14.40	14.80	12.82	9.35	10.87	laser diffraction
37.88	124.27	0.00	0.46	73.34	26.20						0.00	0.00	0.00	0.01	0.46	0.86	7.55	19.19	24.27	21.47	26.20	laser diffraction
38.40	125.98	0.00	0.00	74.08	25.92						0.00	0.00	0.00	0.00	0.00	0.48	7.70	19.81	24.69	21.41	25.92	laser diffraction
39.92	130.98	0.00	1.82	80.66	17.51						0.00	0.00	0.00	0.00	1.82	11.49	19.41	19.32	16.79	13.65	17.51	laser diffraction
41.45	135.98	0.00	2.03	84.18	13.79						0.00	0.00	0.00	0.00	2.03	16.11	24.12	19.28	14.06	10.60	13.79	laser diffraction
42.97	140.98	0.00	1.86	78.59	19.55						0.00	0.55	0.28	0.00	1.03	10.45	18.17	17.95	17.29	14.73	19.55	laser diffraction
44.50	145.98	0.00	2.75	81.64	15.61						0.00	0.00	0.00	0.00	2.75	15.93	21.30	17.75	14.81	11.85	15.61	laser diffraction
46.02	150.98	0.00	3.00	84.17	12.83						0.00	0.00	0.00	0.00	3.00	21.32	23.97	16.60	12.64	9.63	12.83	laser diffraction
47.54	155.98	0.00	3.47	84.84	11.69						0.00	0.00	0.00	0.00	3.47	21.50	25.25	17.06	12.22	8.80	11.69	laser diffraction
49.97	163.94	0.00	35.13	61.54	3.33						0.00	0.00	0.00	4.22	30.91	35.10	14.97	6.14	3.15	2.18	3.33	laser diffraction
50.59	165.98	0.00	39.01	57.39	3.60						0.00	0.00	0.00	6.67	32.34	31.51	13.97	6.25	3.28	2.37	3.60	laser diffraction
52.32	171.64	0.00	37.29	59.49	3.23						0.00	0.00	0.00	5.92	31.37	32.81	14.95	6.50	3.10	2.13	3.23	laser diffraction
53.74	176.31	0.00	46.51	50.57	2.92						0.00	0.00	0.00	10.83	35.68	28.06	12.17	5.53	2.79	2.01	2.92	laser diffraction
55.16	180.98	0.00	58.61	39.10	2.30						0.00	0.00	0.00	18.51	40.10	22.47	8.79	4.02	2.18	1.64	2.30	laser diffraction
56.69	185.98	0.00	58.92	39.04	2.03						0.00	0.00	0.00	15.58	43.34	24.60	7.70	3.41	1.86	1.48	2.03	laser diffraction
58.21	190.98	0.00	69.38	28.56	2.05						0.00	0.00	0.69	27.85	40.84	15.55	6.18	3.12	2.07	1.64	2.05	laser diffraction
59.64	195.66	0.00	39.91	57.35	2.74						0.00	0.00	0.00	5.63	34.29	34.31	13.47	5.20	2.54	1.83	2.74	laser diffraction
61.26	200.98	0.00	86.80	12.38	0.82						0.00	0.00	3.89	44.86	38.05	6.85	2.68	1.09	0.95	0.80	0.82	laser diffraction
62.68	205.66	0.00	96.60	3.40							0.40	0.80	34.60	55.30	5.60	3.40						sieve
64.31	210.98	0.10	96.80	3.10						0.10	0.60	1.00	36.50	53.20	5.50	3.10						sieve
65.83	215.98	0.00	94.20	5.80							0.20	0.30	25.10	57.60	11.00	5.80						sieve
67.56	221.64	4.30	91.20	4.60				1.10	1.30	1.80	3.20	41.60	33.10	9.50	3.80	4.60						sieve
68.88	225.98	10.40	87.50	2.10			6.20	0.70	0.70	2.70	6.20	24.00	50.10	5.00	2.10	2.10						sieve
70.40	230.98	69.20	30.70	0.10			23.50	12.10	16.30	17.30	14.70	8.00	5.20	2.00	0.90	0.10						sieve
71.93	235.98	72.60	25.80	1.60		5.90	32.40	17.10	10.20	7.00	4.60	6.00	11.60	2.40	1.10	1.60						sieve
74.98	245.98	14.70	79.80	5.40			2.90	3.10	4.20	4.50	1.70	5.90	29.10	31.40	11.70	5.40						sieve
77.92	255.66	75.10	23.40	1.50			58.70	9.20	4.80	2.40	4.40	8.50	4.60	3.50	2.30	1.50						sieve
81.07	265.98	37.00	62.40	0.60			2.80	7.40	13.80	13.00	6.20	9.80	27.10	16.80	2.50	0.60						sieve
84.12	275.98	84.30	14.70	1.00		8.40	20.90	27.10	16.50	11.40	5.00	2.20	2.30	3.50	1.60	1.00						sieve
87.77	287.95	6.00	91.30	2.70				3.20	2.50	0.30	0.10	1.30	23.80	56.10	10.10	2.70						sieve
90.62	297.30	69.00	25.80	5.20		12.70	16.30	20.10	14.10	5.70	1.40	1.40	3.30	10.30	9.30	5.20						sieve
92.74	304.27		2.69	85.57	11.73						0.00	0.00	0.00	0.01	2.68	11.09	17.32	21.66	21.03	14.48	11.73	laser diffraction
94.26	309.27		11.69	82.45	5.86						0.00	0.00	0.00	0.02	11.68	33.04	23.88	12.59	7.76	5.17	5.86	laser diffraction
95.59	313.61		7.81	86.62	5.57						0.00	0.00	0.00	0.00	7.81	32.68	27.68	13.03	8.03	5.21	5.57	laser diffraction
96.21	315.66		9.33	86.16	4.51						0.00	0.00	0.00	0.02	9.31	35.23	27.93	12.15	6.79	4.06	4.51	laser diffraction
97.84	320.98	65.10	32.30	2.70		11.50	13.90	17.40	13.40	8.90	5.30	5.90	9.60	8.30	3.10	2.7						sieve
100.88	330.98	70.40	27.90	1.80			16.20	28.20	14.50	11.50	7.10	6.30	7.80	4.90	1.80	1.8						sieve
103.93	340.98	0.20	99.30	0.50						0.20	6.10	70.10	20.50	1.70	0.90	0.5						sieve
106.16	348.28		22.96	68.75	8.29						0.00	0.00	0.00	4.05	18.92	16.08	12.10	14.92	14.99	10.66	8.29	laser diffraction
106.88	350.66		5.28	82.39	12.33						0.00	0.51	0.39	0.14	4.24	12.04	15.19	19.39	20.67	15.10	12.33	laser diffraction
108.40	355.66		51.43	42.26	6.31						0.00	0.00	0.00	13.16	38.27	19.58	7.69	5.65	4.87	4.48	6.31	laser diffraction
110.03	360.98	57.70	40.40	1.90		14.50	10.90	14.00	9.00	9.20	10.60	19.60	6.20	2.40	1.70	1.90						sieve
111.45	365.66		1.43	87.66	10.91						0.00	0.50	0.34	0	0.59	10.5	21.76	21.89	20.1	13.42	10.91	laser diffraction
112.98	370.66		4.73	86.00	9.27						0.00	0.00	0.00	0.002	4.73	22.28	21.31	16.45	15.46	10.51	9.27	laser diffraction
114.50	375.66		8.06	81.54	10.40						0.00	0.00	0.00	0.21	7.85	19.34	17.3	16.92	16.31	11.67	10.4	laser diffraction
115.40	378.61	6.50	86.00	7.40				2.40	2.70	1.50	1.50	13.40	34.20	22.50	14.40	7.40						sieve
117.55	385.66	76.10	23.00	0.90		27.40	16.80	16.00	8.50	7.30	8.40	9.40	3.10	1.20	1.00	0.90						sieve

Table A3-1. ***Willshire-21 clay and silt XRD analysis table showing raw peak data and calculated mineral percentages.***

Willshire-21	Clay (<63µm) Minerals Data XRD Analysis														Silt and Sand (8-63µm) Minerals Data XRD Analysis										
	Peak Height in CPS (Counts Per Second)					Mineral Content (Background Removed)					Chlorite-kaolinite calculation (using MgEG scans)				Peak Height in CPS (Counts Per Second)						Mineral Content (Background Removed)				
	S	V	I	K+C		Smectite	Vermiculite	Illite	Kaolinite	Chlorite		Peak intensity (Background Removed)			Qtz	K-spar	Plag	Calcite	Dolomite						
Depth (ft)	**1.7 nm**	**1.4 nm**	**1.0 nm**	**0.72 nm**	**Sum**	**% S**	**% V**	**% I**	**% K**	**% C**	**% K+C**	**24.9 2-Θ (%K)**	**25.1 2-Θ (%C)**	**Sum**	**3.34Å**	**3.25Å**	**3.20Å**	**3.04Å**	**2.89Å**	**Sum**	**% Qtz**	**% K-spar**	**% Plag**	**% Calcite**	**% Dolomite**
17	0	371	2020	2156	12480	0.0	4.2	64.7	10.4	20.7	31.1	1279	2534	3813	7060	251	516	1566	1925	17700	39.9	5.7	10.2	18.1	26.1
27	0	437	2183	2294	13473	0.0	4.5	64.8	9.6	21.0	30.6	1181	2576	3757	6239	202	580	1617	1758	16611	37.6	4.9	12.2	20.0	25.4
42	0	327	2083	1996	12383	0.0	3.7	67.3	8.8	20.3	29.0	905	2091	2996	5467	173	450	1201	3927	19621	27.9	3.5	8.0	12.5	48.0
67	88	274	1346	1603	8776	1.4	4.4	61.3	12.5	20.3	32.9	1012	1642	2654	7039	278	528	1104	3363	20333	34.6	5.5	9.1	11.1	39.7
77	97	317	1532	1657	9690	1.4	4.6	63.2	11.3	19.5	30.8	1036	1789	2825	7247	335	488	1154	3627	21366	33.9	6.3	8.0	11.1	40.7
87	242	451	2583	2410	15640	2.2	4.0	66.1	11.7	16.1	27.7	1884	2591	4475	7606	233	450	1412	2595	19236	39.5	4.8	8.2	15.0	32.4
97	187	428	1554	1792	10303	2.5	5.8	60.3	13.6	17.7	31.3	1504	1959	3463	5807	192	215	968	1471	12842	45.2	6.0	5.9	15.5	27.5
144	63	191	1054	983	6341	1.4	4.2	66.5	11.8	16.1	27.9	746	1012	1758	7429	169	324	969	4740	22601	32.9	3.0	5.0	8.8	50.3
152	121	278	1939	1738	11443	1.5	3.4	67.8	11.2	16.2	27.3	1277	1852	3129	7392	205	259	1199	3402	19741	37.4	4.2	4.6	12.5	41.4
172	103	304	1832	1779	11100	1.3	3.8	66.0	11.7	17.2	28.8	1450	2132	3582	7312	150	225	1068	3611	19555	37.4	3.1	4.0	11.2	44.3
192	233	459	2841	2646	17096	1.9	3.8	66.5	11.2	16.6	27.9	1785	2637	4422	7882	187	307	1154	2845	18898	41.7	4.0	5.7	12.5	36.1
212	118	347	2462	2157	14382	1.1	3.4	68.5	11.3	15.7	27.0	1663	2322	3985	8588	249	343	1187	3133	20737	41.4	4.8	5.8	11.7	36.3
227	296	413	2105	1884	12804	3.2	4.5	65.8	10.6	15.9	26.5	1482	2236	3718	8245	290	304	1016	3115	20028	41.2	5.8	5.3	10.4	37.3
297	145	465	2758	2895	17097	1.2	3.8	64.5	12.8	17.6	30.5	2571	3534	6105	9347	225	248	730	2312	18160	51.5	5.0	4.8	8.2	30.6
307	271	450	2760	2659	16836	2.3	3.7	65.6	11.2	17.2	28.4	1945	2972	4917	9435	260	345	691	2341	18717	50.4	5.6	6.5	7.6	30.0
317	225	460	2592	2620	16043	2.0	4.0	64.6	11.6	17.8	29.4	1954	2994	4948	8939	233	307	993	2280	18453	48.4	5.1	5.8	11.0	29.7

Figure A3-1. Willshire-21 clay and silt mineralogy plots.

Table A3-2. ***Domestic clay and silt XRD analysis table showing raw peak data and calculated mineral percentages.***

Domestic	Clay (<63µm) Minerals Data XRD Analysis														Silt and Sand (8-63µm) Minerals Data XRD Analysis										
	Peak Height in CPS (Counts Per Second)					Mineral Content (Background Removed)					Chlorite-kaolinite calculation (using MgEG scans)				Peak Height in CPS (Counts Per Second)						Mineral Content (Background Removed)				
	S	V	I	K+C		Smectite	Vermiculite	Illite	Kaolinite	Chlorite		Peak intensity (Background Removed)			Qtz	K-spar	Plag	Calcite	Dolomite						
Depth (ft)	**1.7 nm**	**1.4 nm**	**1.0 nm**	**0.72 nm**	**Sum**	**% S**	**% V**	**% I**	**% K**	**% C**	**% K+C**	**24.9 2-Θ (%K)**	**25.1 2-Θ (%C)**	**Sum**	**3.34Å**	**3.25Å**	**3.20Å**	**3.04Å**	**2.89Å**	**Sum**	**% Qtz**	**% K-spar**	**% Plag**	**% Calcite**	**% Dolomite**
22	68	414	1875	2080	11919	0.8	4.9	62.9	11.1	20.3	31.4	1221	2228	3449	5892	280	474	1488	3008	18941	31.1	5.9	8.8	16.1	38.1
37	0	372	1911	2135	12008	0.0	4.3	63.7	10.0	22.0	32.0	988	2181	3169	5283	217	443	1344	3532	18934	27.9	4.6	8.2	14.6	44.8
52	0	476	2556	2353	15126	0.0	4.4	67.6	9.9	18.1	28.0	1424	2595	4019	5186	333	508	1547	3081	18862	27.5	7.1	9.4	16.8	39.2
67	68	360	2102	2238	13036	0.7	3.9	64.5	9.6	21.3	30.9	1135	2511	3646	5179	246	470	1517	2966	18036	28.7	5.5	9.1	17.2	39.5
80	50	364	2284	2230	13730	0.5	3.7	66.5	10.0	19.3	29.2	1295	2503	3798	5531	186	440	1436	3024	18016	30.7	4.1	8.5	16.3	40.3
97	80	413	1663	2683	12172	0.9	4.8	54.7	18.3	21.4	39.7	2219	2590	4809	7529	351	661	816	3381	21034	35.8	6.7	11.0	8.0	38.6
107	138	347	1450	1850	9809	2.0	5.0	59.1	13.8	20.2	33.9	1289	1889	3178	6150	275	576	983	4209	21383	28.8	5.1	9.4	9.4	47.2

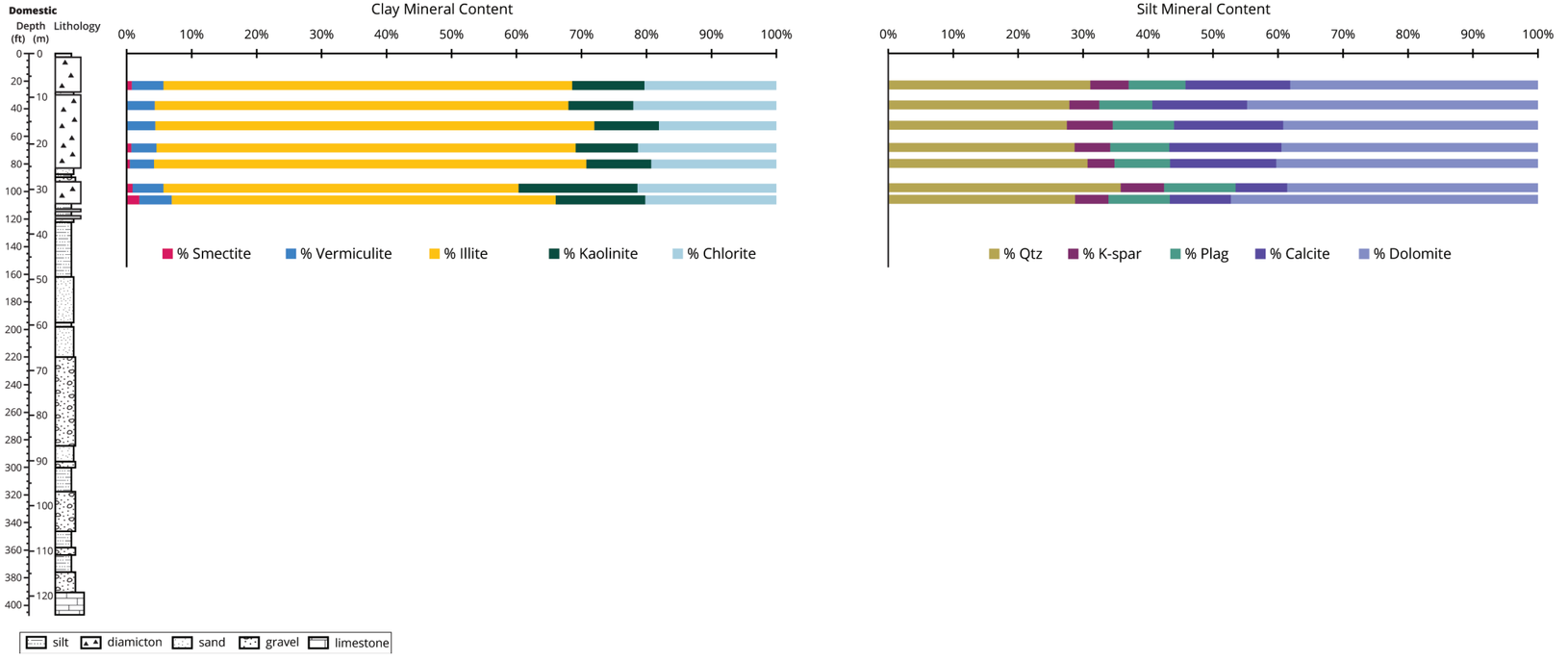

Figure A3-2. Domestic clay and silt mineralogy plots.

APPENDIX 4
Optically Stimulated Luminescence Data

All elemental data available upon request. IGWS-ID is the internal lab number for OSL analysis, referred in figures labeled according to sample ID.

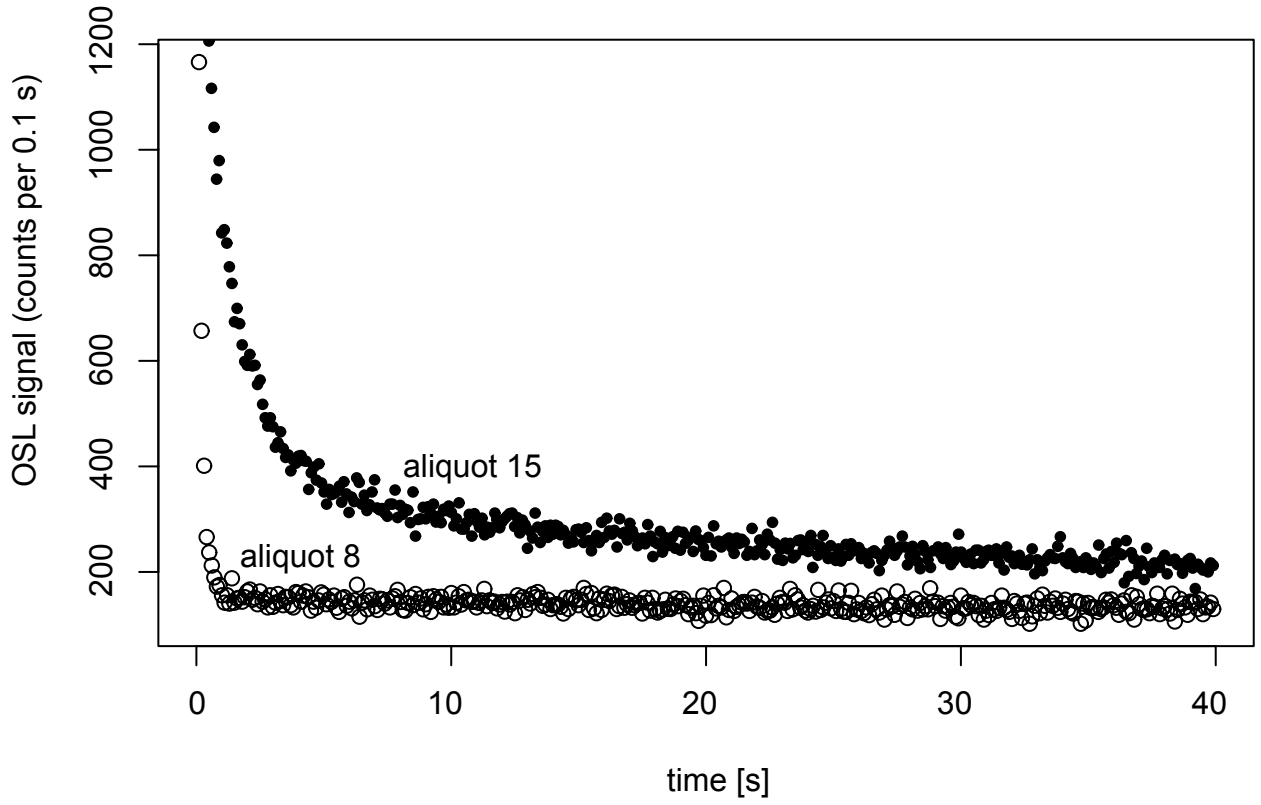

Figure A4-1. Comparison of OSL signal components for aliquots of sample IGWS-405 (Willshire-21 core), after irradiation with ~25 Gy. Aliquot 8 (open symbols) is dominated by a fast component evident by the rapid decay of signal after 1 second of illumination with 100 mW/cm2 of blue light. Aliquot 15 (closed symbols) is dominated by slow and medium components which tend to decay slower and can be unstable at geological timescales. A commonly used indicator for acceptance of an aliquot is the fast ratio of Durcan and Duller (2011), which can be quantified from the measurements in the plot and instrumental parameters. The higher the ratio the better, with a threshold of ~20 for accepting aliquots. The fast ratio for aliquot 8 is ~40, compared to ~5 for aliquot 15.

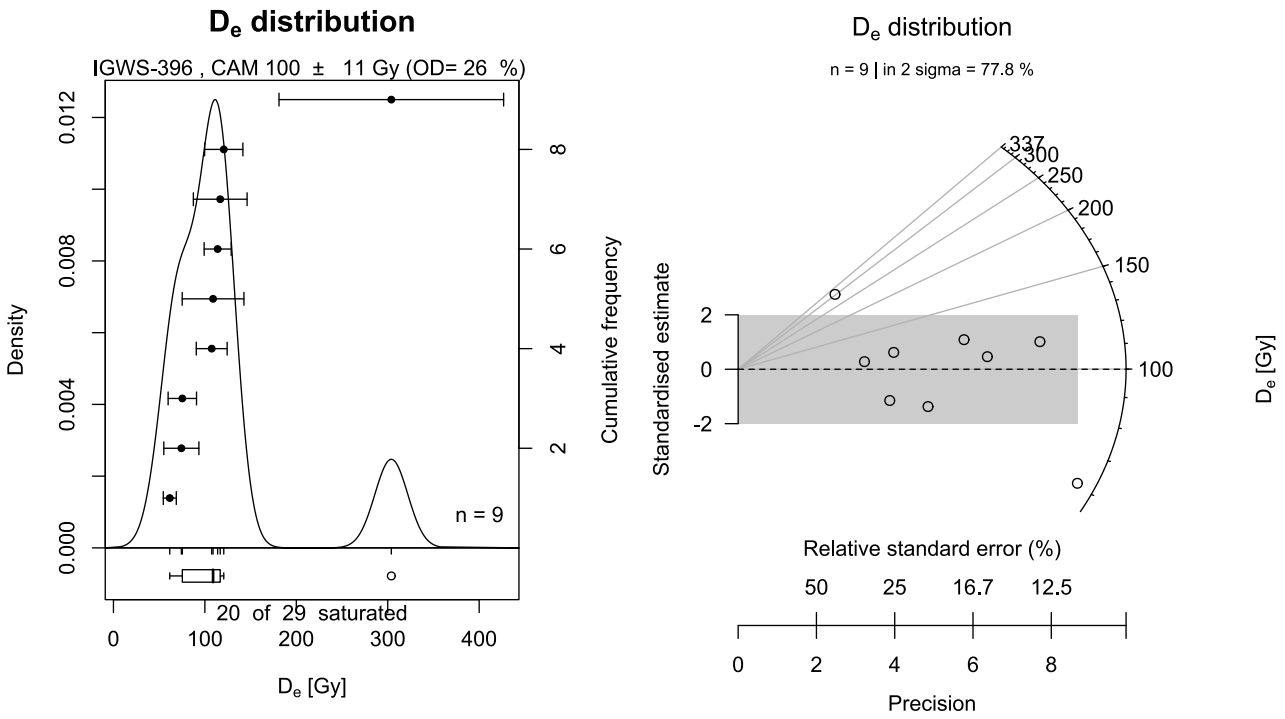

Figure A4-2. IGWS-396. Domestic, 380–385 ft sample. Age: 77 ± 10 ka using a CAM estimate of De = 100 ± 11 Gy. Overdispersion: 26%. Saturated = 20/29; 11 aliquots weak or displaying slow/medium signal.

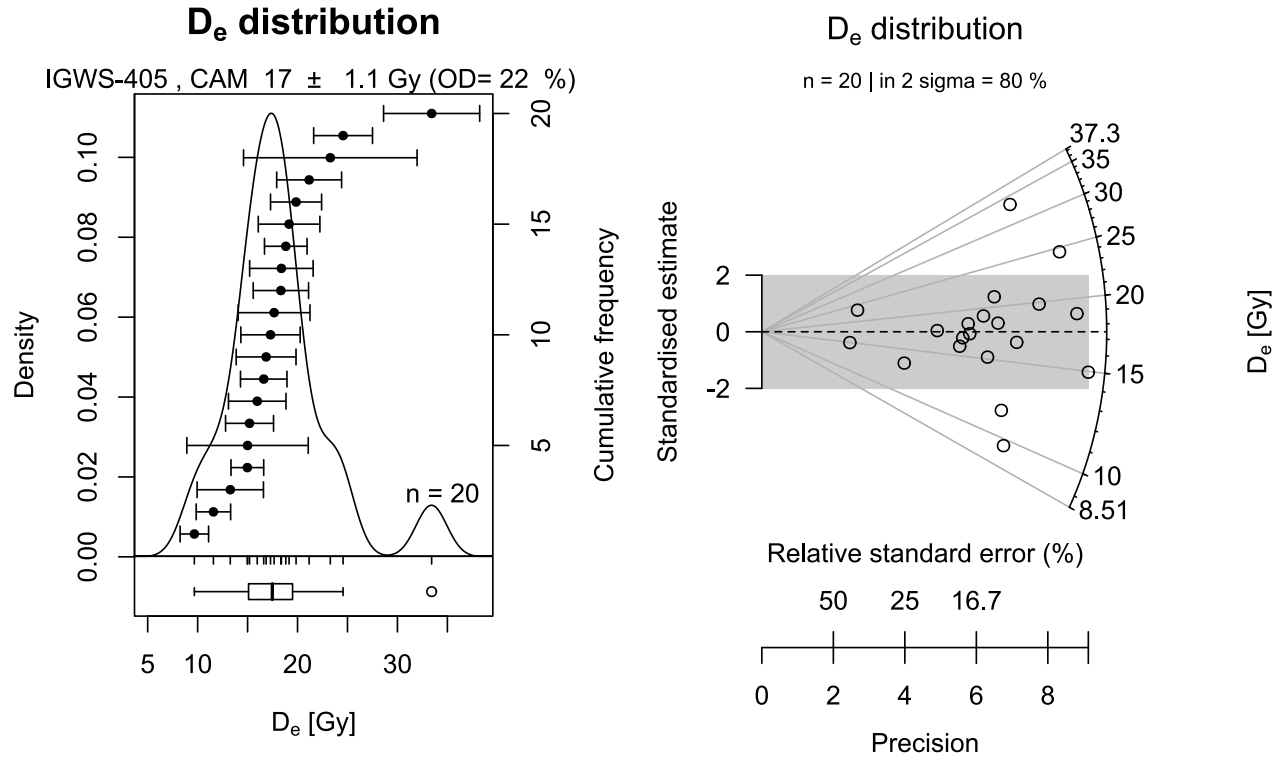

Figure A4-3. IGWS-405. Domestic, 85–90 ft sample. Age: 15.8 ± 1.6 ka using a CAM estimate of De = 17 ± 1.1 Gy. Overdispersion: 22%.

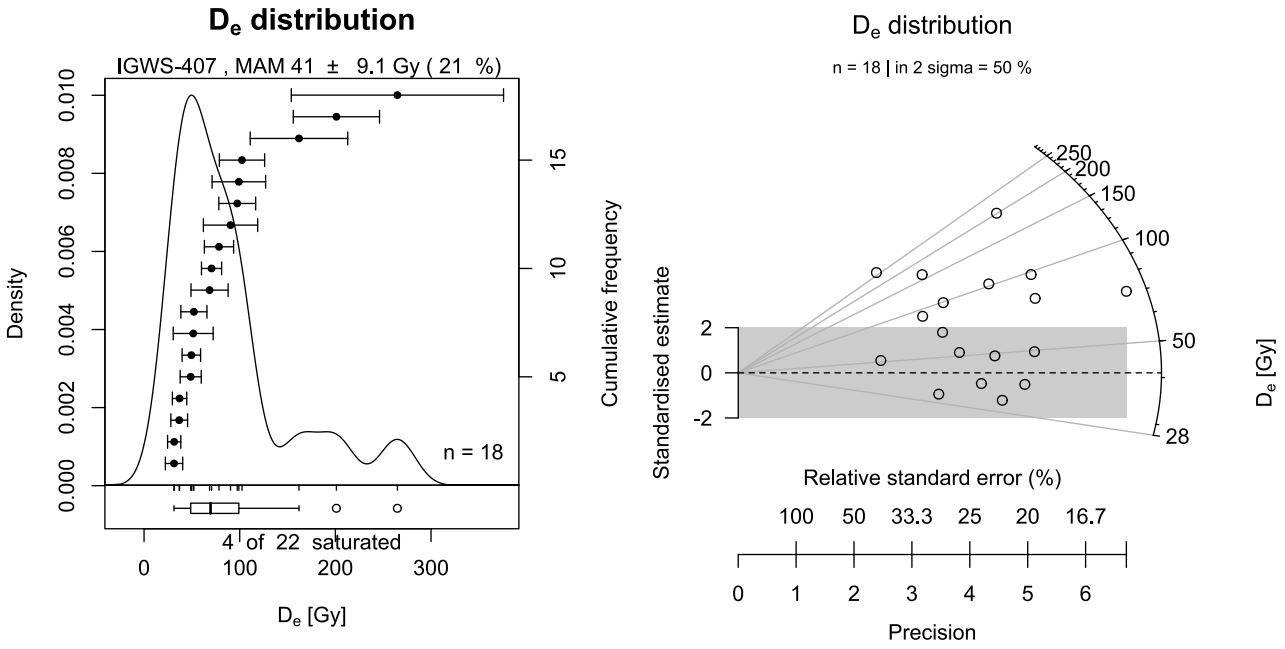

Figure A4-4. IGWS-407. Willshire-21, 65 ft sample. Age: 49 ± 14 ka using a MAM estimate of De = 41 ± 9 Gy. Model overdispersion: 21%.

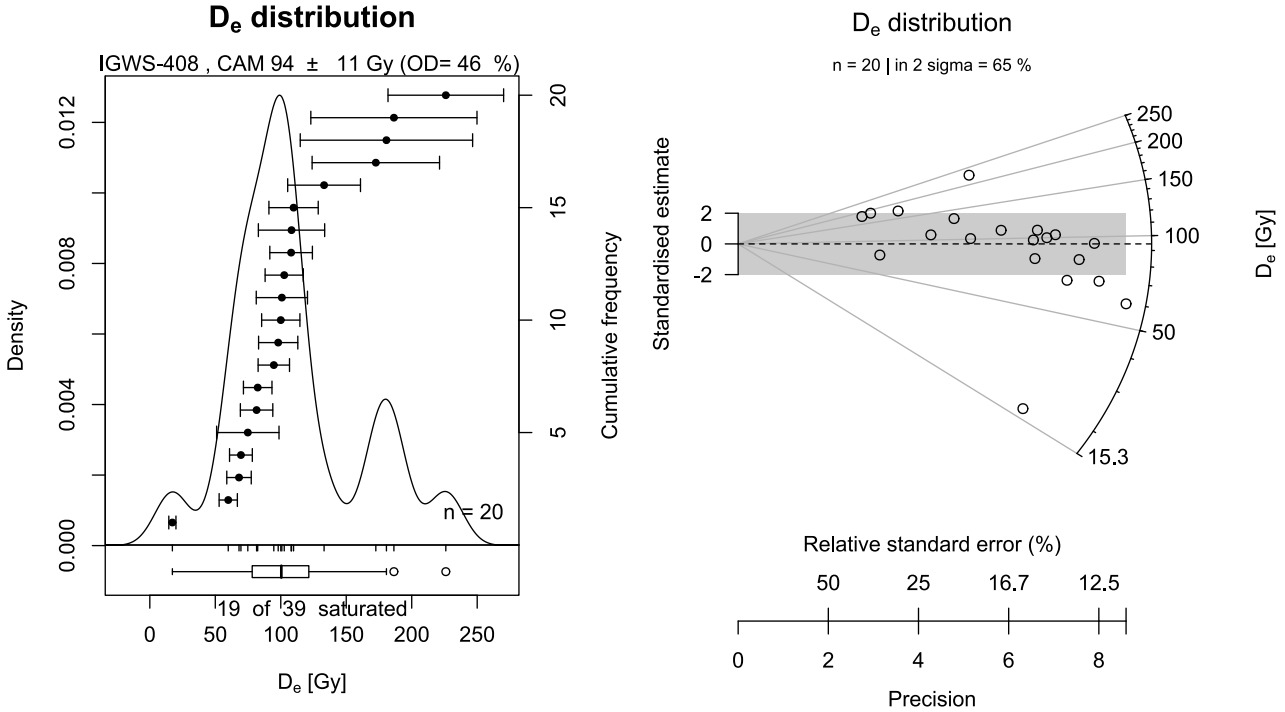

Figure A4-5. IGWS-408. Willshire-21, 245 ft sample. Age: 79 ± 11 ka using a CAM estimate of De = 94 ± 11 Gy. Overdispersion: 46%.

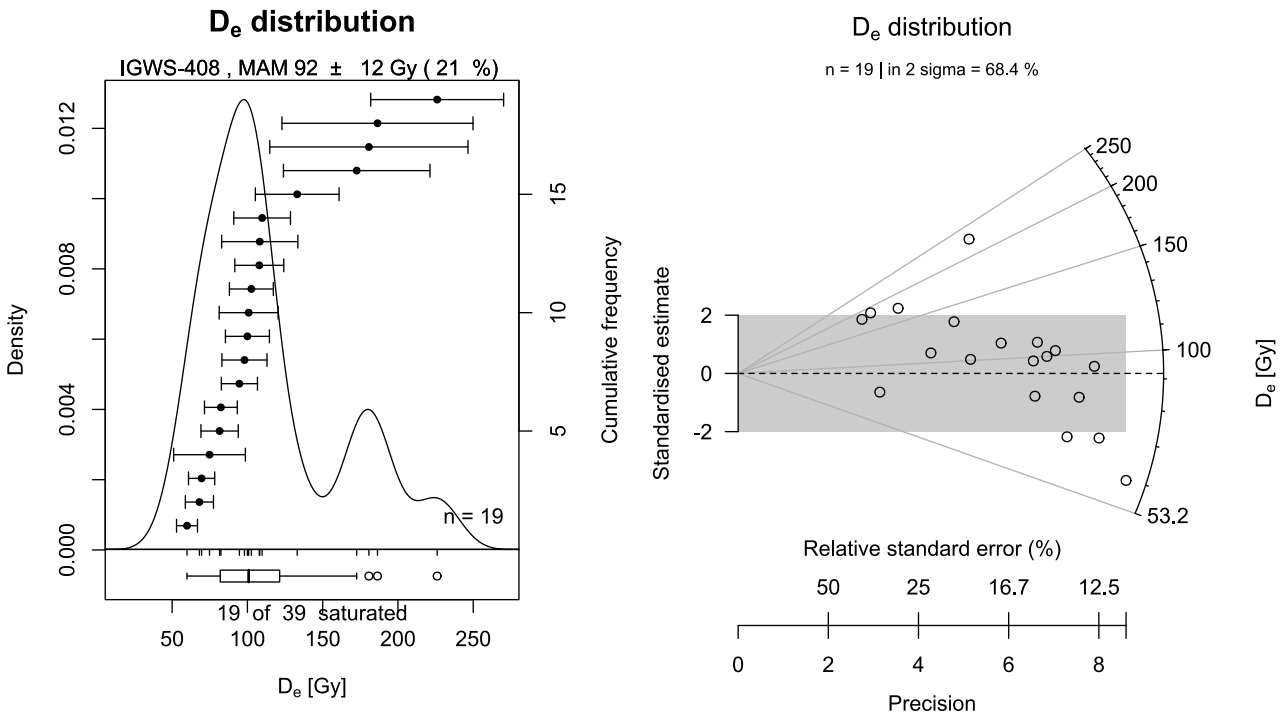

Figure A4-6. IGWS-408. Willshire-21, 245 ft sample. Age: 78 ± 11 ka using a MAM estimate of De = 92 ± 12 Gy, and not considering the youngest measured aliquot. Model overdispersion: 21%.

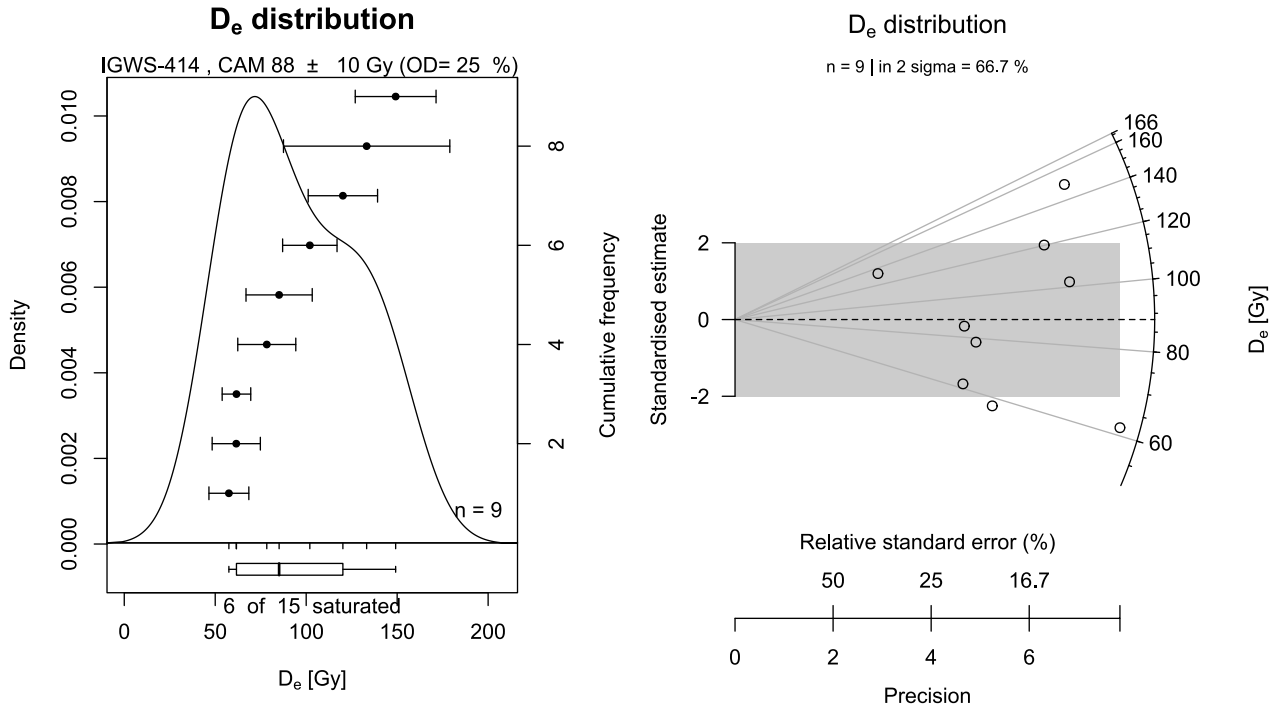

Figure A4-7. IGWS-414. Willshire-21, 325 ft sample. Age: 67 ± 9 ka using a CAM estimate of De = 88 ± 10 Gy. Overdispersion: 25%.

This page intentionally left blank

OHIO GEOLOGICAL SURVEY
DEPARTMENT OF NATURAL RESOURCES

(614) 265-6576 • geo.survey@dnr.ohio.gov
geology.ohiodnr.gov